Introduction to Porphyrins and Tetrapyrroles

November 23, 2021

Contents

1 General Introduction **1**

2 Nomenclature of Tetrapyrroles **2**

3 Relevance in Nature **4**

3.1 Heme 4

3.2 Biliverdin and Bilirubin 7

3.3 Phycobilisomes and Phytochromes 8

4 Synthetic Aspects **9**

4.1 Free-Base Porphyrins 9

4.1.1 Unsubstituted Porphyrin (Porphin) 11

4.1.2 *meso*-Tetrasubstituted Porphyrins 11

4.1.3 Octa-β-Substituted Porphyrins 12

4.1.4 D_{2h}-Symmetric Porphyrins 13

4.1.5 MacDonald Condensation 14

4.2 Metal Porphyrins 14

4.2.1 Stability Classes 14

4.2.2 Five Step Model 16

4.2.3 Preparation Methods 17

5 Properties **20**

5.1 Optical Spectra 20

5.1.1 Absorption Spectra 21

5.1.2 Emission Spectra 24

5.1.3 Regular and Irregular Porphyrins 25

5.2 Infrared Spectra 26

5.3 Mass Spectra 26

5.4 ^{1}H-NMR Spectra 27

6 Reactivity of the Porphyrin Ring **29**

6.1 Electrophilic Aromatic Substitution (S_EAr) 29

6.2 Nucleophilic Aromatic Substitution (S_NAr) 30

6.3 Ring Cleavage 30

7 Bilindiones and Biliverdins **31**

7.1 Bilindiones 31

7.2 Biliverdins 34

7.3 Properties 35

8 Current Trends in Porphyrin Science **36**

8.1 Molecular Electronics 36

8.1.1 Biladienones as Molecular Switches 36

8.1.2 Vanadyl Porphyrins as Qubits 38

8.2 Structural Chemistry: Nonplanar Porphyrins 38

8.3 Catalysis: Carbene Transfer Reactions 39

8.4 Nonlinear Optics of Tetraphenylporphyrin 39

9 Supplementary Information **47**

1 General Introduction

Porphyrins belong to the group of tetrapyrroles and are both abundantly found in nature as well as – thanks to their intriguing structure and properties – in the laboratories dedicated to various fields within science. This manuscript should serve as the more thorough basis for the underlying presentation. Trying to make this into a mini-review is necessarily futile: A brief search for "porphyrin" in the *ISI Web of Knowledge* reveals that the publication output has grown from 106 publications in 1971 to a staggering 2,584 publications in 2020. Moreover, the probably most comprehensive book series about the field to date – the Handbook Of Porphyrins – is an absolute behemoth in all regards, spanning forty-four volumes (and costing roughly 16.000 USD or 1.4 mio JPY for all printed books!). Thus, it is only reasonable to assume that a handful of fields might have gotten under the radar — and that is not even considering that there exists an entire journal dedicated to porphyrins and phthalocyanines.

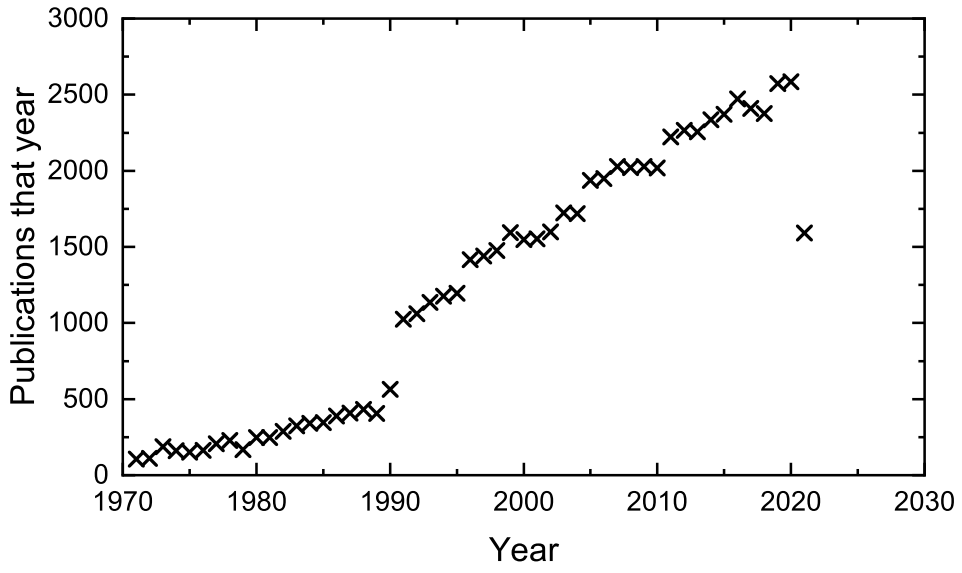

Figure 1: Search results containing "porphyrin" in Clarivate Analytic's "ISI Web of Knowledge", sorted by year. The entry for the year 2021 on the far left is preliminary as of mid-September 2021.

Giving up the attempt to write even a "micro-review" and aiming for something several orders of magnitude smaller, this manuscript will introduce the reader to some roles of porphyrins in nature and its biosynthesis. Afterwards, the most well-studied man-made porphyrins are introduced, along with their synthesis and key properties. As complexation of a metal ion leads to a drastical change in physicochemical properties, some metal complexes of porphyrins are introduced afterwards, in a similar fashion. From here, the scope is slightly opened up by dedicating a brief section to some linear tetrapyrroles and their metal complexes. Lastly, some current research trends in the field of porphyrins and tetrapyrroles are shown. However, a brief part of this work has to be dedicated to nomenclature beforehand, as to avoid confusion later on.

2 Nomenclature of Tetrapyrroles

The nomenclature of porphyrins typically follows the one proposed by Fischer, Orth and Stern in their monograph, *Die Chemie des Pyrrols* [1] [2] [3] (engl. *The Chemistry of Pyrrole*). As becomes apparent from Figure 2 below, five structural motifs make up the reference points for the further naming of compounds: Porphin and porphyrinogen from which porphin (or porphine) can be *gen*erated. Chlorin (or 7,8-Dihydro-21H,23H-porphin) is derived from the *chlor*ophylls in which the motif can easily be recognized. Similarly, *bacterio*chlorin points to special chlorophylls that can be found in organisms such as cyano*bacteria*: These bacteriochlorophylls carry one less double bond and – contrary to the chlorophylls – do not produce oxygen as a byproduct of photosynthesis. Phorbin resembles the structure of chlorin with an additional cyclopentane ring fused to the methine group and two of the pyrrole carbons.

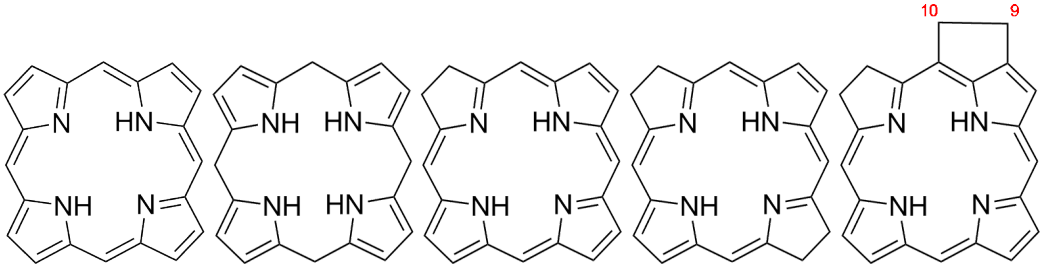

Figure 2: Structures of prominent tetrapyrroles. From left to right: Porphin, porphyrinogen, chlorin, bacteriochlorin, phorbin. For phorbin, additional position numbers are given according to Fischer nomenclature.

A later revision of by the *Commission on the Nomenclature of Biological Chemistry* in 1960 [4] led to the 1–24 numbering scheme (see Figure 3) as well as the nomenclature for any side chains, while mostly retaining most of the trivial names embraced by Fischer nomenclature.

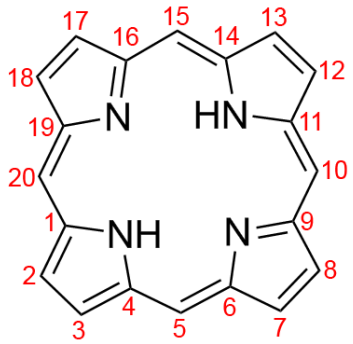

Figure 3: Numbering scheme of substituents in porphyrins.

In the case of D_{4h}-symmetric porphyrins (neglecting the N–H bonds of the free base), a simpler nomenclature has prevailed because of its high symmetry: The carbon atoms in the pyrrole rings are referred to as α and β (relative to the nitrogen atoms), and the carbon atoms at the methine bridge are referred to as being *meso*.

3 Relevance in Nature

3.1 Heme

The most prominent heme, heme b, is synthesized in nature starting from the glycine and succinyl-CoA in the mitochondrion [5]. In 1945, Shemin *et al.* found that intake of ^{15}N-labelled glycin leads to radioactively labeled nitrogen atoms of the heme. Using ^{14}C-labelling methods, they also found that eight of the carbons in the porphin macrocycle originated from the α-carbon in glycin. Lastly, use of ^{14}C-labelled acetate revealed that the remaining 26 carbon atoms originate from acetate: Twenty-four from the methyl and two from the carboxyl carbon.

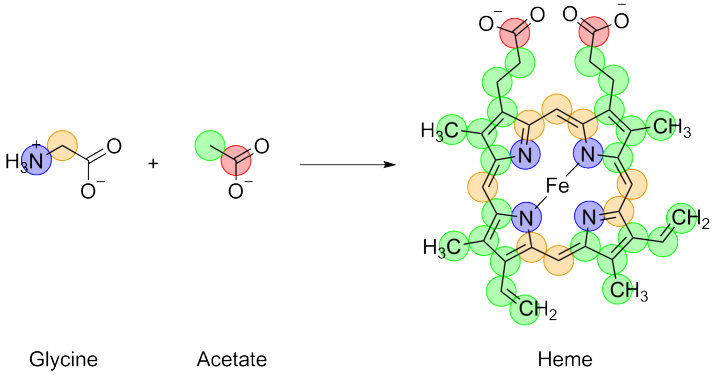

Figure 4: Origin of the nitrogen and carbon atoms in heme, as found by Shemin *et al.*

This lead to the hypothesis that heme b has to be synthesized from condensation of glycin with some sort of acetate donor (perhaps an activated succinyl compound):

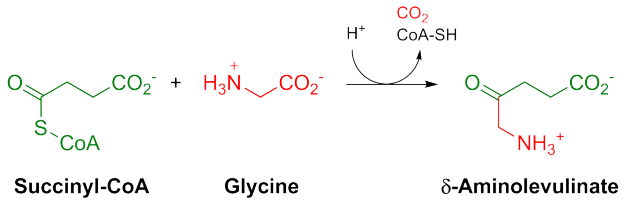

From here, the pathway is as follows [6]: In a second step, two of these resulting δ-aminolavulinates undergo a condensation reaction to porphobilinogen. This reaction is catalyzed by the enzyme δ-aminolavulinate-dehydrase. The resulting product is porphobilinogen (PBG):

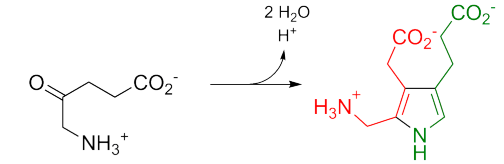

In the next reaction, PBG deaminase condenses four of these pyrrole derivates condense into a linear tetrapyrrole. Ring closure leads to the formation of uroporhyrinogen III (UPG III):

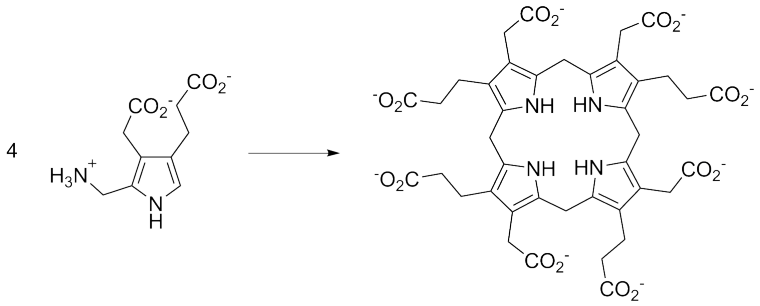

UPG-III-decarboxylase then cleaves the ethanoate groups to form coproporhpyrinogen III (CPG III):

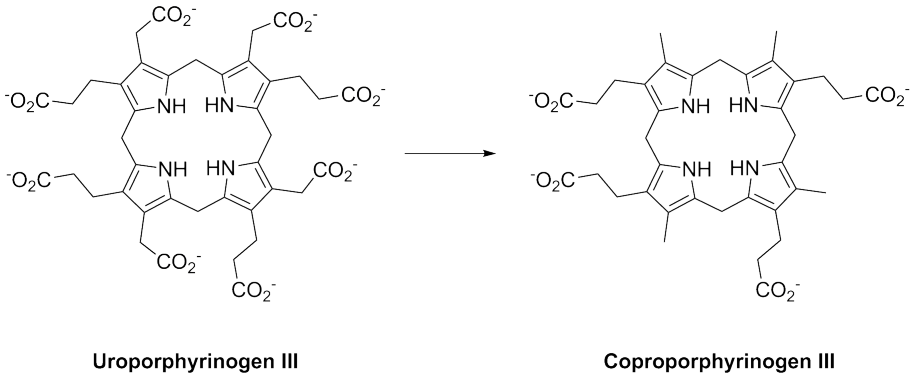

Similarly, the enzyme CPG-III-oxidase partially decarboxylates the propionate groups to give vinyl groups:

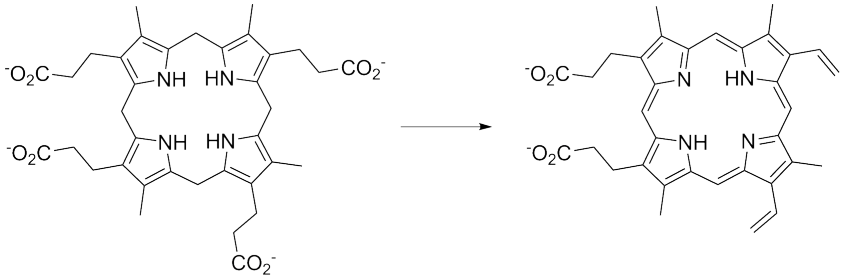

Coproporphyrinogen III **Protoporphyrin IX**

In the last step, the protoporphyrinogen IX (PPG IX) is oxidized by PPG oxidase. The product is the heme molecule as a free base. Chelation with iron, for example, can now be either achieved with transferrin (Fe^{3+}) or with ferrochelatase (Fe^{2+}). In both cases, the resulting iron is provided by ferritin.

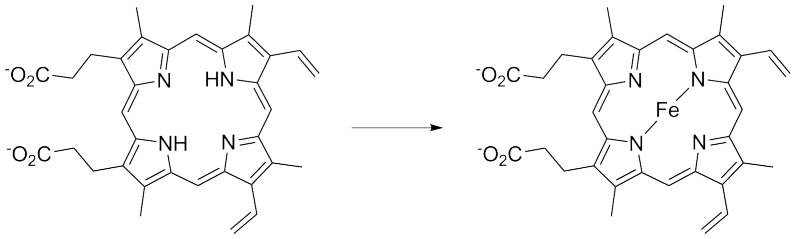

Protoporphyrin IX **Heme**

3.2 Biliverdin and Bilirubin

Death of the erythrocytes commences the heme catabolism, in which the first step is the oxidative cleavage of an α-methine group by the enzyme *heme-oxygenase*. In this reaction, NADPH is used as a cofactor and serves as the reductand.

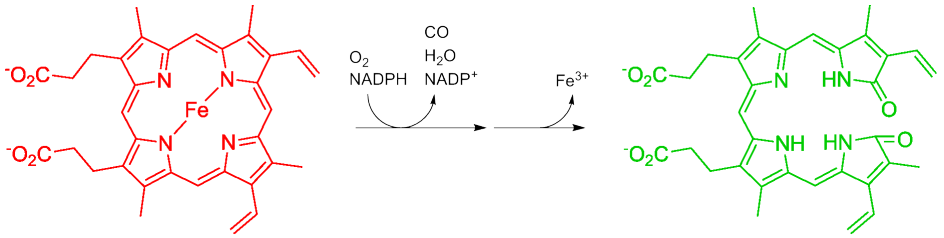

Heme **Biliverdin**

The resulting biliverdin, a green-yellow compound, is reduced by *biliverdin reductase* to give the red bilirubin.

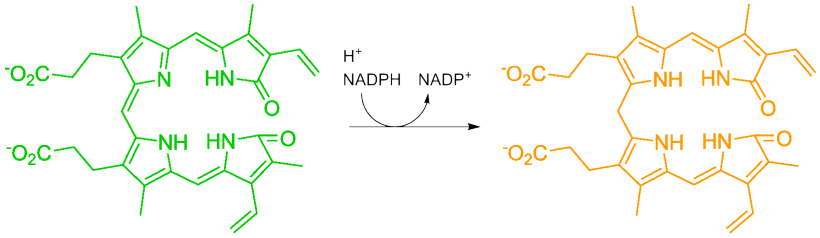

Biliverdin **Bilirubin**

Healing of a bruise or a hickey is an everyday example of this part of heme catabolism. Bound to the serum albumin, the biliverdin is first transported to the liver and then to the bile (hence its name), where it is excreted via the gastrointestinal tract and, to a smaller extent, via urine. Bilirubin was also found to be a very effective antioxidant (close to vitamin E), whereas biliverdin is not. Together with ascorbate (vitamin C) and urate, bilirubin it belongs to the three most important antioxidants in human blood serum.

3.3 Phycobilisomes and Phytochromes

In photosynthesis, a process employed by plants living above the water surface, chlorophyll aids in the synthesis of plant matter from carbon dioxide and water. Under water however, the wavelengths absorbed by chlorophyll (red and blue light) are transmitted less and less as the depth of the water increases. Here, cyanobacteria and algae have adapted to use protein complexes located at the cell membranes (the *phycobilisomes*) to harvest light in the region between 470 nm and 650 nm. The energy derived from photoexcitation is then transferred to phycobiliproteins and later to the chlorophyll in the active site of the photosystem II.

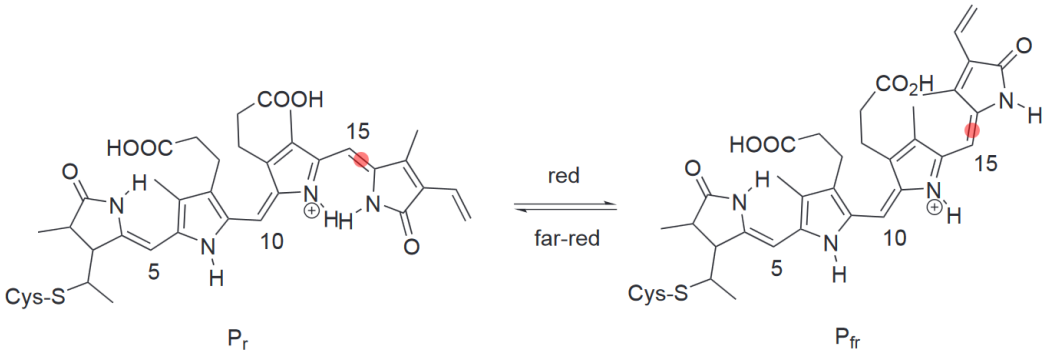

P_r P_{fr}

Figure 5: Photoisomerization of the phytochromobilin in the protein phytochrome. *Cys* denotes a cystein unit in the rest of the protein. The bond experiencing photoisomerization is highlighted in red.

In plants living above the water surface, biliproteins known as *phytochromes* (Figure 5) are commonly found. The tetrapyrrole in their active site – bound to the rest of the molecule via a thioether linkage – exhibits two different structural isomers that can be interconverted by light in the region of 660 nm and 730 nm. Commonly referred to as the P_r/P_{660} and the P_{fr}/P_{730} form, these molecules resemble nature's own *photoswitches*: In the dark and during the night, only the physiologically inactive P_r is produced. As the sun rises and the plant is exposed to 660 nm light, P_r is converted into P_{fr}. This conformational change leads to structural changes in other parts of the protein, and enhances several physiological functions such as the growth of leaves or RNA synthesis. As the sun sets, the presence of 660 nm light vanishes and the produced P_{fr} is converted back into P_r by light in the far red region (770 nm).

4 Synthetic Aspects

4.1 Free-Base Porphyrins

Of course, nature has had tens of thousands of years to develop specialized, high-yield catalysts in the form of enzymes. On the other hand, the synthetic organic chemist does not enjoy these amenities and instead has to face several challenges. One of them is the formation of insoluble black polymer material. From a purely retrosynthetic point of view, the synthesis seems straightforward: The porphyrin ring can be retrosynthetically "cut" into four subunits based on pyrroles and aldehydes which should easily undergo condensation (driven by the formation of an aromatic system.) As of now however, there is no procedure that entirely prevents this reaction from going beyond the *tetra*pyrrole: Most reactions either produce staggering amounts of insoluble polymer material or they have to be employed as sophisticated multi-step reactions with highly sensible intermediates and/or starting materials.

A second problem that mainly concerns the synthesis of natural porphyrins has been described in literature as the *type-isomer problem* (Figure 6). These types of porphyrins – such as heme B – have an asymmetric substitution pattern so that, if a condensation approach from pyrroles were used, the pyrroles have to carry different substituents on the two β-positions. The problem is then to prevent these pyrrole units from "facing the wrong way".

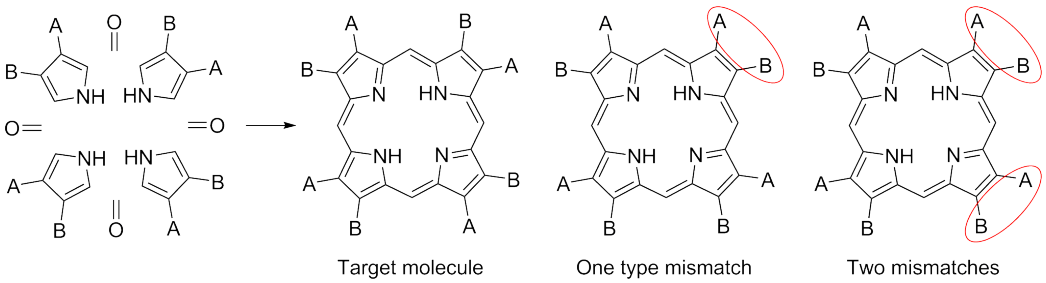

Figure 6: The type-isomer problem shown for the case of a porphyrin with only substituents named "A" and "B".

As is apparent at this point, the synthesis of naturally occuring porphyrins is a science as much as it is an art. For the interested reader, a very intriguing synthesis

is the total synthesis of chlorophyll *a* by Robert Burns Woodward in 1960. If still not convinced, a thorough study of the total synthesis of cobalamin (Vitamin B_{12}) is recommended, which was achieved by Albert Eschenmoser at the ETH Zürich and Woodward in 1972, in a joint research effort.

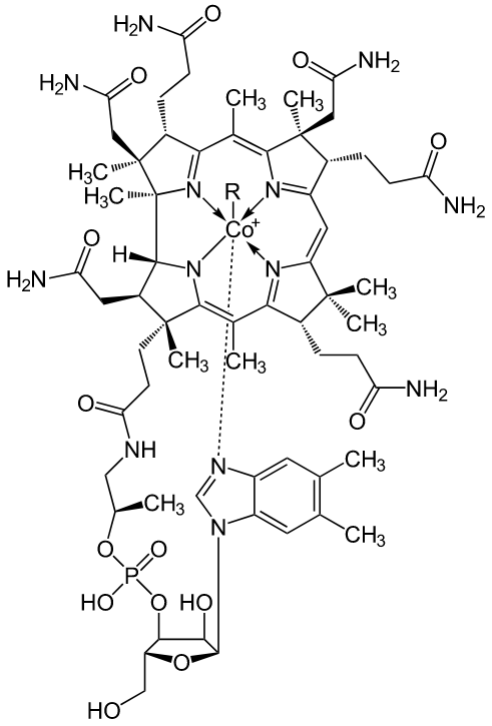

Figure 7: General structure of the cobalamins. In Vitamin B_{12}, R=5'-Desoxyadenosyl.

The mere fact that this work involved over a combined 100 chemists and 16 years of research [7] should be telling enough about its complexity. For the sake of this manuscript however, we will skip these synthesis as well as the synthesis of natural tetrapyrroles entirely. Detailed reviews about this synthesis – such as one by Eschenmoser himself [8] – can be found elsewhere [9]. Instead, we will concern ourselves with much simpler substitution patterns that can be found in the man-made porphyrins.

4.1.1 Unsubstituted Porphyrin (Porphin)

While the first isolation of heme dates back as far as 1867 (by Thudichum, who treated hemoglobin with sulfuric acid [10]), the first synthesis of the *unsubstituted* porphin followed more than fifty years later by Hans Fischer (awarded with the Nobel Prize in Chemistry in 1930) who used pyrrole-α-aldehyde in formic acid [11]. The yield was very low and first made it to single-digit percentage after the work of Steffan Krol, who prepared porphin from 2-hydroxymethylpyrrole with potassium persulfate in glacial acetic acid [12]. In 1997, yields of porphin would make it into the double-digits when Ellis and Langdale used a two-phase approach: The two phases consist of water acidified with acetic acid and the immiscible 4-methyl-2-pentanone. With the 2-hydroxymethylpyrrole and subsequent oxidation of the resulting porphyrinogen with dichlorodicyanoquinone (DDQ), the reaction gave a yield of 15.3 % [13]. In the same year, Taniguchi *et al.* published a study that doubled the yield to 31 % [14]. Here, 2,5-bis(hydroxymethyl)pyrrole is first synthesized from pyrrole and formalin, and then further treated with excess pyrrole under acidic conditions to give tripyrrane. This tripyrrane is condensed with pyrrole, using $BF_3{\cdot}OEt_2$ as a Lewis acid catalyst to give porphyrinogen. Finally, oxidation with DDQ gives porphin. However, this reaction still has to find broad application to date, as both the hydroxypyrrole and the tripyrrane are sensitive to light, air and temperatures above $5\,^{\circ}\mathrm{C}$. Another promising synthesis was published by Neya *et al.* in 2002 [15] who used a deprotection strategy: Starting from 5,10,15,20-tetrakis(*tert*-butyl)porphin, acidic de-*tert*-butylation with equal volumes of concentrated sulfuric acid and *n*-butanol gave porphin in 74 % yield. The alkylporphin itself can be readily prepared from pyrrole and pivalaldehyde (*tert*-butylformaldehyde) in 15 % yield, leading to an overall yield of 11.1 %.

4.1.2 *meso*-Tetrasubstituted Porphyrins

As of the time of writing this manuscript, the reaction conditions employed by Lindsey *et al.* in 1987 [16] are seemingly the most reliable for *meso*-tetrasubstituted symmetric porphyrins. In this case, pyrrole is reacted with a suitable aldehyde in the presence of either $BF_3{\cdot}OEt_2$ or TFA as an acid catalyst. In a subsequent step, DDQ is then used to oxidize the resulting porphyrinogen to the desired porphyrin.

When $BF_3{\cdot}OEt_2$ is used, triethyl orthoacetate may be used as a water scavenger to drive the yield as high as 50–55 % in the case of *meso*-tetraphenylporphyrin [7]. One downside of this reaction is that it depends on good solubility of all reagents in CH_2Cl_2. As a result, porphin may not be synthesized under Lindsey conditions, as it would involve using the insoluble paraformaldehyde. Moreover, sterically hindered aldehydes such as mesitaldehyde or pivalaldehyde seem to have a harder time reacting under these conditions, lowering the yield significantly. Nonetheless, this *Lindsey condensation* can be used to synthesize the *tert*-butylporphyrin mentioned in the section above.

4.1.3 Octa-β-Substituted Porphyrins

Similarly to *meso*-tetrasubstitution, the high symmetry of octa-β-substituted porphyrins facilitates their synthesis by eliminating the type-isomer problem mentioned earlier. The introduction of substituents, again, also greatly improves the solubility, making handling and characterization much easier when compared to porphin, which has a strong tendency to form π-aggregates [17].
As it shares the most similarities with the naturally occuring hemes, octaethylporphyrin (OEP) is probably among the porphyrin compounds with the widest interest in past and current research, together with *meso*-tetraphenylporphyrin. First synthesized by Fischer and Bäumler in as early as 1928 [4], a more modern synthesis of OEP from Sessler *et al.* is given in Figure 8 [18].

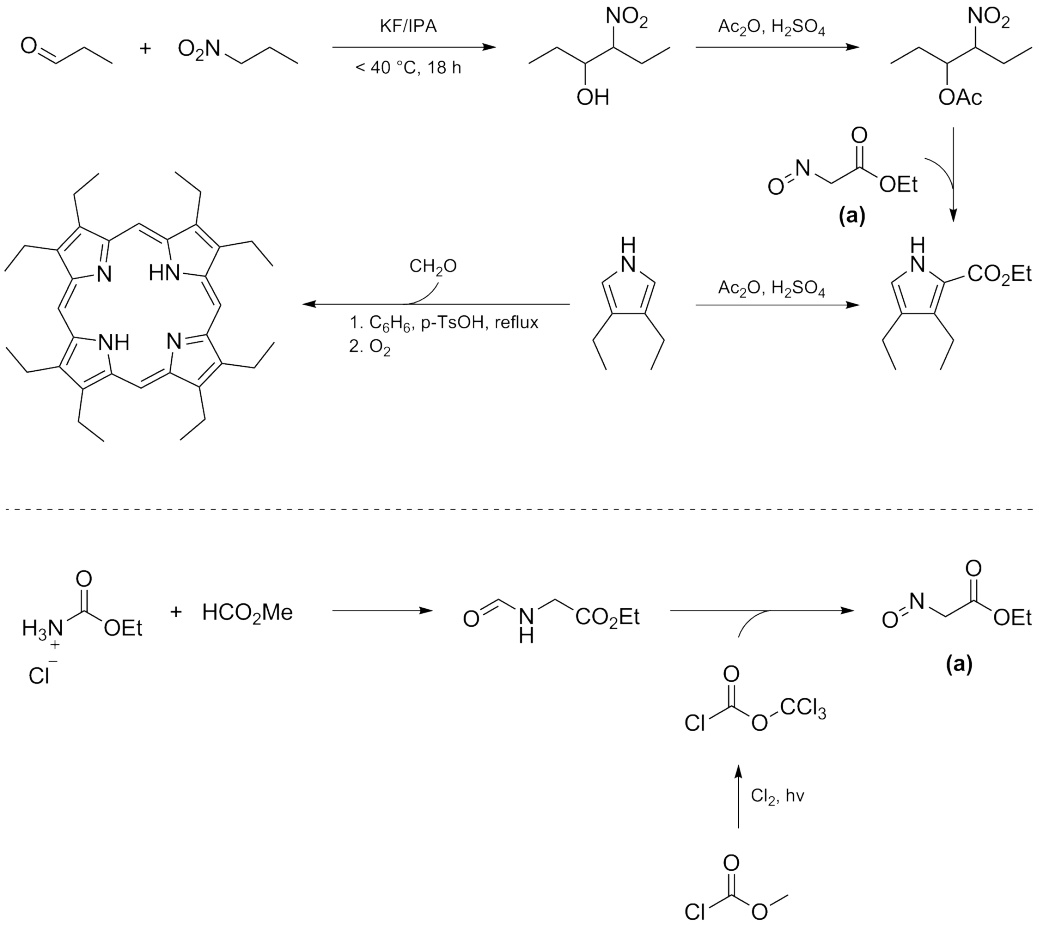

Figure 8: Synthesis of octaethylporphyrin (OEP) by Sessler *et al.*

The synthesis, while enabling the synthesis of OEP on a gram-scale (theoretically, 56 g of OEP from the product of the first step), has its bottleneck in the foul-smelling and fairly expensive ethyl isocyanoacetate. This compound may be synthesized in three steps if one does not mind the extra commitment, and the mild inconvenience of working with chlorine gas.

4.1.4 D_{2h}-Symmetric Porphyrins

If the target porphyrin is D_{2h}-symmetric and has AB-substituted pyrrole subunits, a synthesis from 3,4-substituted pyrroles is possible even if these substituents are not identical. Smith *et al.* managed to solve the type-isomer problem – otherwise a dealbreaker in this scenario – by using a pyrrole with a leaving group in one of the

α-positions. This leaving group (–NEt_2) could be cleaved under neutral conditions to give coproporphyrin I tetramethyl ester [19].

4.1.5 MacDonald Condensation

If porphyrins of opposite substitution patterns are required, the MacDonald cyclo-condensation may be used. The general approach here is always similar: Exploit the nucleophilicity of the pyrrole ring to join it with a pyrrole structure carrying an aldehyde group to give di-, tri- and lastly tetrapyrroles under acidic conditions. This approach has been used extensively by K. M. Smith and his colleagues, for example to give uroporphyrin II octamethyl ester [20]. In this case of the MacDonald condensation, special care (such as acid-free handling and storage) is needed to avoid self-condensation of the intermediates, and the pyrrole scrambling that leads to the type-isomer problem remains an unresolved issue.

4.2 Metal Porphyrins

4.2.1 Stability Classes

The insertion of a metal atom from a salt MX_n into the porphyrin structure always requires the removal of the two nitrogen-bonded protons. The result is the release of an acid HX which, depending on its strength, may shift the reaction equilibrium towards the educt side completely. It was observed that this demetalation is not only dependent on the acid strength, but also on the metal atom that is incorporated into the porphyrin "pocket" (for example, the size). Hence, the concept of *stability classes* was proposed, which is based purely on empirical findings. These stability classes rank the metal complexes according to their resistance towards acids, and their definition can be taken from Table 1. A "Periodic Table of Metalloporphyrins" is given in the supplementary. This table summarizes the elements incorporated into the porphyrin structure to date, along with their predominant stability class[1].

[1]Based on J. W. Buchler in chapter 10 of D. Dolphin's "The Porphyrins: Volume I. Structure and Synthesis, Part A". Academic Press New York 1978.

Table 1: Definition of the different stability classes of metal porphyrins.

Stability Class	**Behavior at 25 °C after 2 h**
I	Not demetalated by conc. H_2SO_4
II	Demetalated by conc. H_2SO_4
III	Demetalated by HCl
IV	Demetalated by HOAc
V	Demetalated by H_2O

In order to predict these stability classes, a stability index S_i was proposed later on, taking the metal ion's charge-to-radius ratio Z/r and its electronegativity E_n into account:

$$S_i = \frac{Z \cdot E_n}{r} \tag{1}$$

While this approach may be helpful in some cases, it does not consider the structure of porphyrin ligands. This is quite important, as different substituents can alter the both the geometrical and the electronic structure (by steric repulsion, inductive effects, perturbations by additional ligands etc.): This is, for example, reflected in the different stability of [Sb(OEP)]Cl and [Sb(OEP)(OH_2)]ClO_4 with stability class III and I, respectively. Furthermore, electrochemical properties and the absolute size of the metal atom are not considered: think, for example of Cr(III) or Hg(II), respectively. As a consequence, the concept of stability indices may give some right predictions, but shows a handful of inconsistencies when compared to impirical findings; It can only be considered an "educated guess" with gross oversimplifications and a narrow scope of applications.

4.2.2 Five Step Model

In order to properly incorporate the metal M into any porphyrin structure P, all synthetic routes have to overcome a multitude of individual steps. In the example of $[Cr^{III}P(OPh)](PhOH)$ prepared from $Cr_2(acac)_3$, these are as follows:

1. **Shifting of the protonation/deprotonation equilibrium**:
   $H_4P^{2+} \rightleftharpoons H_3P^{+} \rightleftharpoons H_2P \rightleftharpoons HP^{-} \rightleftharpoons P^{2-}$

2. **Dissociation of the metal from its carrier**:
   $Cr_2(acac)_3 \rightleftharpoons 2\ Cr^{3+} + 2\ acac^{2-}$

3. **Association of metal and porphyrinato ions**:
   $Cr^{3+} + P^{2-} \rightleftharpoons CrP^{+}$

4. **Charge compensation by ligand association**:
   $CrP^{+} + PhOH \rightleftharpoons [CrP(OPh)] + H^{+}$

5. **Filling the coordination sphere**:
   $[CrP(OPh)] + PhOH \rightleftharpoons [CrP(OPh)](PhOH)$

Note that, while the first three steps are mandatory in all cases, the fourth and fifth are only necessary if the metal ion carries a charge larger than two (step 4) and ifs preferred coordination number is not four. In the light of these different subreactions within porphyrin metalation, the choice of metal carrier and solvent seems nontrivial, as metal salts, ligands and porphyrins used may hold their individual caveats. Hence, a variety of metalation procedures has been developed, with some of them introduced in the next section.

4.2.3 Preparation Methods

Acetate Method

As the name implies, the metal carrier in this procedure is a metal acetate such as $Zn(OAc)_2 \cdot 2\ H_2O$ and the solvent is typically glacial acetic acid. This method is generally applicable to all divalent metals under the caveat that the resulting metal porphyrin complex is not attacked by acetic acid (stability class III or higher).
One example of this method is the preparation of zinc(II)-etioporphyrin I:
This procedure is also used fairly often in transmetalation of magnesium tetrapyrroles with transition metals: both for porphyrins and for bilindiones and biliverdins (which are introduced later).

$$Zn(OAc)_2 \cdot 2\ H_2O + H_2(\text{Etio-I}) \xrightarrow[100\ ^\circ C,\ 1\ h]{HOAc} Zn(\text{Etio-I}) + 2\ HOAc + 2\ H_2O$$

Pyridine Method

In the case of acid-labile complexes, pyridine can be used as a reaction medium. The advantage here lies in the basic nature of pyridine which can easily "buffer" the liberated acid HX, as it is present in large excess compared to the reactants. This may come at the cost of generating complexes with pyridine ligands which are not always desired and/or easy to remove. In addition, the good coordination abilities of pyridine may lead to longer reaction times or incomplete reaction if higher-charged metal cations should be incorporated.
This method was successfully employed to synthesize $Mg(OEP)(Py)_2$, where magnesium assumes an octahedral coordination sphere:

$$Mg(ClO_4)_2 + H_2(OEP) + 4\ Py \xrightarrow[\text{Darkness, Reflux, 14 h}]{\text{Pyridine}} Mg(OEP)Py_2 + 2\ PyH^+ + 2\ ClO_4^-$$

The resulting complex can be stripped of its pyridine ligands by washing with 0.1 M HCl, which leaves the otherwise acid-sensitive Mg(OEP) untouched.

Acetylacetonate Method

This method is especially promising due to the weak acidity of the liberated acetylacetone ($pK_s \approx 9$), making more acid-labile complexes accessible. The

solubility of acetylacetonates in many solvents, along with their availability even for more exotic metals like palladium are other advantages. However, low acidity of the acetylacetone also means a high stability of the acetylacetonates, making it necessary to use weakly acidic solvents the PhOH. Metal ions of high charge-to-radius ratio may also suffer from a rather labile coordination sphere if this approach is used.
In the case of metals in the scandium and the boron row, the lanthanides and some early transition metals, the acetylacetonate method is the method of choice. Consider, for example, the following reaction:

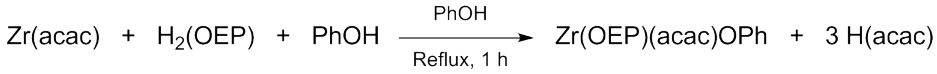

Phenoxide Method

Using metal oxides or chlorides in boiling phenol is characteristic for the phenoxide method. This is typically the case for a handful of metal acetylacetonates that are not reactive enough for the previous reaction, such as Ta, Mo, W, Re. As a general rule, most metals accessible through the acetylacetonate method are also accessible through this method.
High concentrations seem to facilitate this reaction, as in the example of $Ta(OEP)F_3$, which was prepared in two steps, first from $TaCl_5$ and then by treatment with HF and MeOH:

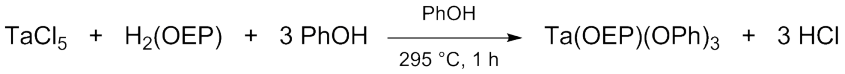

Benzonitrile Method

Some metal halides form aggregates that are very hard to "break apart" so that they are hard to access chemically or to get into solution. This problem can be solved by using benzonitrile as a solvent, which has a high boiling point of $191\ ^\circ\mathrm{C}$ so that reactions of higher temperatures are accessible. An added advantage of the high temperature is that it allows for the liberated HX to evaporate, using Le Chatelier's principle to drive the reaction towards the product side. However, one needs to take special precaution during this reaction, as the order of adding reagents seems

crucial: In the case of tetraarylporphyrins, the halides have to be added *before* the porphyrins, as it otherwise leads to the formation of green, unstable and unwanted products was observed.
The benzonitrile method is a great choice for the metalation of porphyrins with Pd, Pt or Nb:

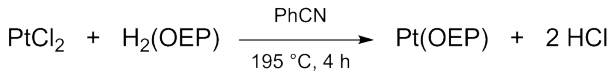

Dimethylformamide Method

Another high-boiling and weakly coordinating solvent is dimethylformamide (DMF). Adler *et al.* used this solvent together with metal halides to access a variety of metal porphyrins, often in quantitative or near-quantitative yield. Oftentimes, the reaction product will readily precipitate out of the solution upon cooling or careful addition of water. If that is not the case, the mixture may be extracted with low-boiling solvents like CH_2Cl_2. However, special attention is needed when choosing the complex to synthesize, as metals that are more stable in higher oxidation states oxidize to there in the course of the reaction (e.g., Cr^{II} to Cr^{III}). Moreover, the metal halides have to be anhydrous and may be difficult to handle, and some metals like tin or magnesium require a tenfold excess of the halide along with long reaction times to go to completion.

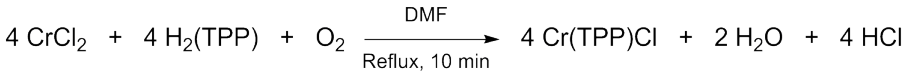

Metal Organyl Method

Metal organyls as metal carriers hold two advantages: The are not only Lewis acidic and thus promote the metal association, but the liberated base is very strong, so that the N-H protons of the porphyrin ring are easily removed. Due to the strong reactivity of metal organyls in general, the handling is one of the method's drawbacks. It also prohibits the use of porphyrins with functional groups other than alkyls.
Using a Grignard-type reaction, the metal organyl method has been used to synthesize magnesium etioporphyrin I as shown below:

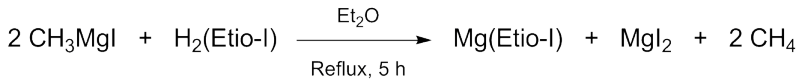

Metal Carbonyl Method

Metal carbonyls can lose one of their CO ligands rather easily, leading to an unsatiated coordination sphere that can associate the porphyrin ligand. This method has been used for metals of the Cr row to the Ni row, such as in the following example:

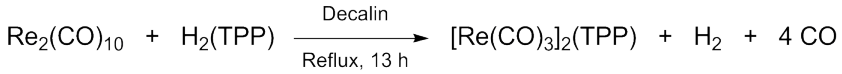

Alkoxide Method

Alkali and rare earth alkali metals, as described earlier, are very labile to acids – even to the point of being demetalated by water. Thus arises the necessity for very basic conditions to keep demetalation to a minimum. Chlorins, compounds closely related to porphyrins, are even more acid-labile and their metalation can be achieved by means of the alkoxide method. The alkoxides can be created *in situ* by alcoholysis of the corresponding Grignard reagents.
An example of the alkoxide method is the metalation of ethyl pheophorbide *a* (a product of chlorophyll catabolism) with magnesium:

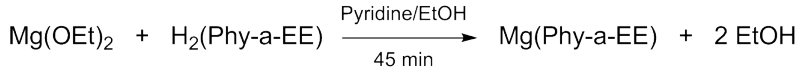

5 Properties

5.1 Optical Spectra

Probably owing to their very intense color – derived from the ancient Greek *porphyra* for "royal purple" – as well as their aromaticity, the electronic properties of porphyrins have been investigated for the better part of a century. The models range from a simple particle-on-a-ring problem and span the Hückel method all

the way until Gouterman's four orbital model and the Pariser-Parr-Pople method which was meant to supplement the Hückel method. The derivation of each method is beyond the scope of the script, but the review in reference [21] may serve as an entry point into the matter. In the following then, only the most characteristic features are being given and several sins of omission have to be committed. In Figure 9, a simplified Jablonski diagram is given for further reference.

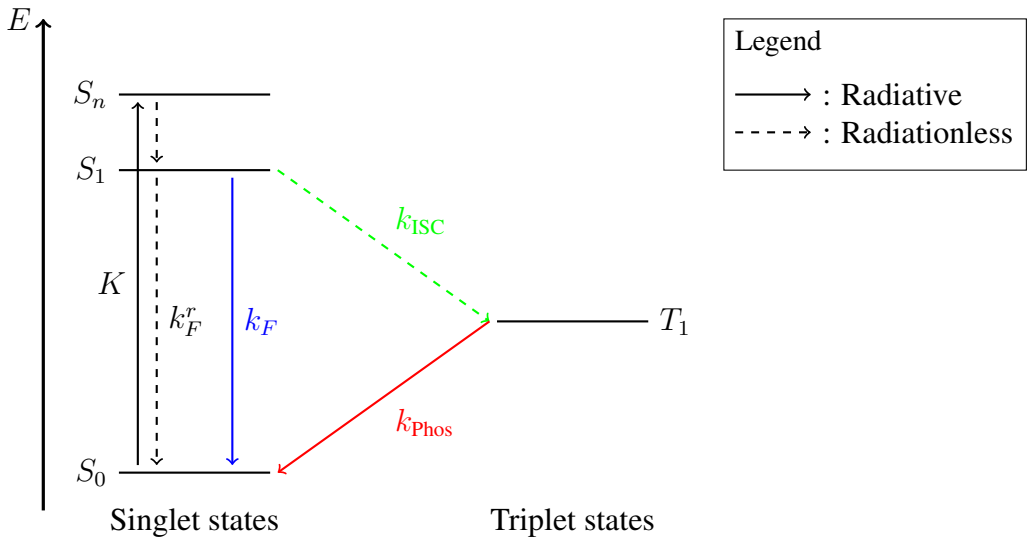

Figure 9: Simplified Jablonski diagram, indicating fluorescence (blue), phosphorescence (red), and intersystem crossing (green) with their respective decay rates k. The triplet state T_1 may also be the result of radiationless decay from a higher-energy triplet state T_{1+n} (internal conversion, not shown).

5.1.1 Absorption Spectra

Most generally, porphyrin spectra show two different bands which follow the nomenclature proposed by Platt *et al.* [22]: Between 500 and 600 nm, two Q bands can be found. These arise from π–π^*-transitions between the electronic ground state S_0 and...

- ... the lowest excited singlet state S_1 (denoted by $Q(0,0)$), or

- ... S_1 with additional vibrational excitation (an "overtone", $Q(1,0)$).

Similarly intense bands that are also referred to as *Soret bands* and denoted by the letter B in Platt nomenclature may be found in the near-UV region between 380 nm and 420 nm. The transition taking place here is between S_0 and...

- ... the second excited singlet state S_2 ($B(0,0)$), or
- ... S_2 with additional vibrational excitation ($B(1,0)$, not always properly resolved).

Further absorption bands are denoted as N, L and M, while the latter is only visible in the vapor phase.

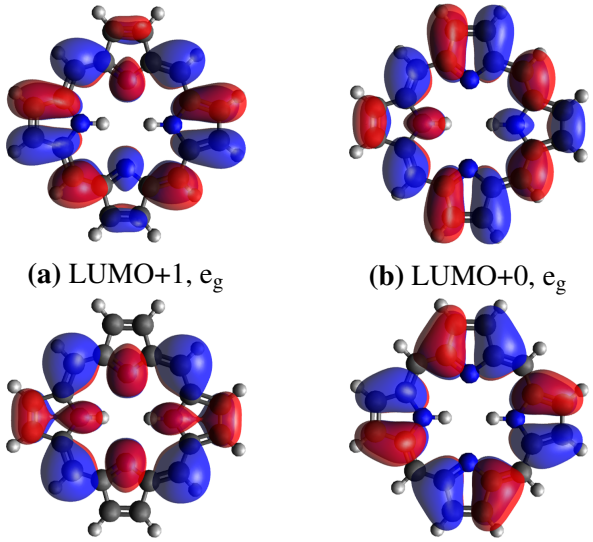

(a) LUMO+1, e_g **(b)** LUMO+0, e_g

(c) HOMO-0, a_{2u} **(d)** HOMO-1, a_{1u}

Figure 10: Structure of the first two LUMOs and the first two HOMOs of porphin, along with their symmetry. Sign indicated by color. Notice how the two HOMOs have four nodal planes, but the LUMOs have five. Calculation in Orca 5.0.0 with DFT using the B3LYP functional with def2-TZVP basis set, and the CPCM method for solvation correction [23] with CH_2Cl_2 as a solvent. Orbitals were rendered in Avogadro 1.2.0 and have an isosurface value of 0.015.

The first two highest occupied and the two lowest unoccupied molecular orbitals of porphin (HOMOs and LUMOs, respectively) are given in Figure 10. Both LUMOs

are strictly degenerate with respect to their energies, as their only difference is a polarization either in x or y direction (keep in mind that these are interchangeable because of resonance). HOMO-0 and HOMO-1, however, are not degenerate but separated in energy.

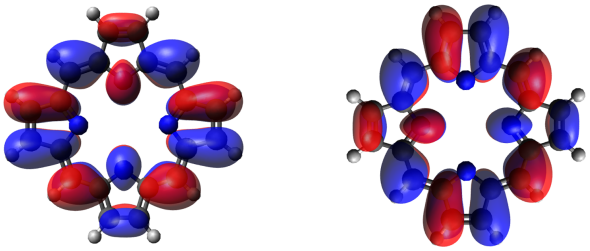

(a) LUMO+1, e_g **(b)** LUMO+0, e_g

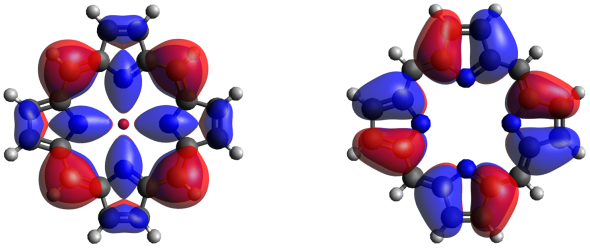

(c) HOMO-0, e_u **(d)** HOMO-1, e_u

Figure 11: Structure of the first two LUMOs and the first two HOMOs of porphinato-magnesium, along with their symmetry. Sign indicated by color, the magnesium atom is left out for clarity. Calculations and rendering according so the same parameters as in Figure 10

Incorporation of another atom into the porphin pocket is only possible if the net overlap between the porphin's MO and the metal's empty p_z orbital is nonzero. Hence, the only possible interaction partner is HOMO-0 with a_{2u} symmetry, and HOMO-1 remains unaffected. As the electropositivity of the incorporated atom increases, the energy of the resulting HOMO-0 decreases and the energy of the resulting HOMO-1 increases: in metals, this is typically up to a point where both HOMO-0 and HOMO-1 are either degenerate or nearly-degenerate. The result is a different mixing behavior of the singlet transitions, when compared to the free base. In short, this difference leads to all absorption bands in free-base porphyrins that contain a transition from HOMO-0 to be split into two different branches: For the Q band, these are Q_x and a Q_y, and for the B band, this is B_x and B_y. Hence, the split bands do not result from any difference in symmetry, but purely from a

difference in energy – an *accidental degeneracy*. This phenomenon is explained in detail by the *Four Orbital Model* proposed by M. Gouterman [24] [25]. The orbitals resulting from metal incorporation are shown in Figure 11. A comparison between the spectra of H_2OEP and Co(OEP) is given in Figure 12.

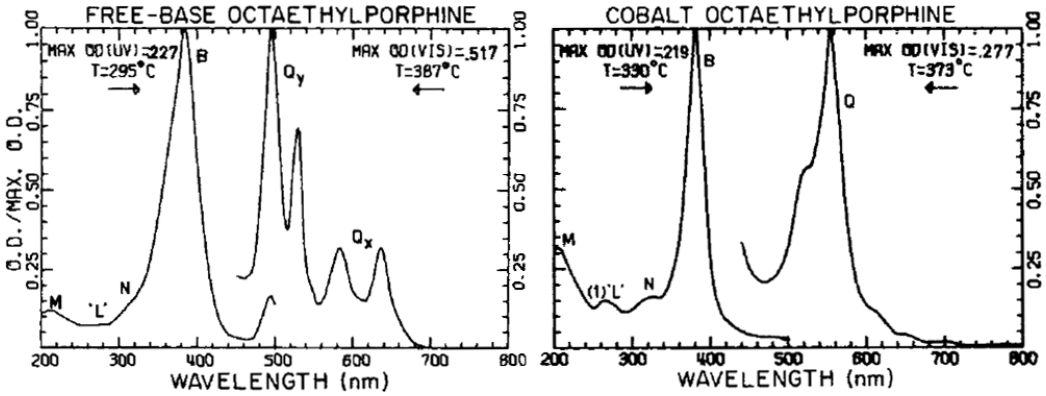

Figure 12: Absorption spectra of H_2OEP and Co(OEP) in the vapor phase [26]. Small amounts of chlorin were added to H_2OEP to enhance the intensities in the far red. Notice the split into $Q_{x,y}$ (and, to a smaller extent, $B_{x,y}$ in the free base).

These characteristic absorptions are observed in all alkyl- and aryl derivatives, and are not affected too much by the nature of the substituent. However, there is a slight trend observable in that the respective bands experience a red-shift compared to the bare porphin. For TPP, this shift is more strongly pronounced than for OEP. Furthermore, in the case of TPP derivatives, different substituent effects arise for *ortho-*, *meta-* and *para*-substitution. Here, it was found that *para*-substitution only had a slight effect on the absorption spectrum, while it was slightly larger in the case of *ortho*-substitution. Carbonyl and vinyl substituents showed a somewhat strong effect, but are still limited in their strength. For these reasons, it is thought that the absorption spectra of the porphyrins is dominated by transitions at the porphin core, not its substituents.

5.1.2 Emission Spectra

As the free-base porphyrins by definition do not coordinate any heavy atoms in the center, their emission spectra show strong fluorescence behavior (high k_F) but very little phosphorescence (low k_{Phos}). Intersystem crossing is reduced as well

(k_{ISC} becomes small) and all processes involving an excited triplet state are less pronounced than in the metallo compounds. Another notable difference is that the natural radiative lifetimes $\tau = k^{-1}$ of the singlet states are longer compared to the metalloporphyrins ($\approx 120\,\mathrm{ns}$ and $\approx 60\,\mathrm{ns}$, respectively).
Upon coordination of a metal atom, fluorescence behavior is less pronounced and phosphorescence increases due to the heavy atom effect.

5.1.3 Regular and Irregular Porphyrins

In the case of metal porphyrins, the metal's electrons may interact with the π electrons of the porphyrin backbone. These interactions – either of electronic or spin-orbit nature – represent perturbations and thus change both absorption and emission spectra. Typically, electronic perturbations are only minor, whereas they are larger for spin-orbit interactions. If the spectrum is mostly perturbation-free, the respective porphyrin is called *regular*, whereas porphyrins with significant perturbations in their spectra are called *irregular*.
Metals forming regular metalloporphyrins are:

- All alkaline and alkaline earth metals
- Group III B: Sc(III), Y(III), La(III), Lu(III)
- Group IV B: Ti(IV), Zr(IV), Hf(IV), Th(IV)
- Group V B: Nb(IV), Ta(V)
- Group II B: Zn(II), Cd(II), Hg(II)
- The entire group III A and IV A (with carbon as an *N*-methyl complex)
- Group V A: P(V), As(V), Sb(V)

Spectra of irregular metalloporphyrins are typically separated into *hypso* and *hyper* spectra. Hypso spectra show a blue shift with respect to the regular spectrum. These types of spectra are observed in complexes with metals of the nickel and copper group, or in transition metals with d^{6-9} where the e_g levels are completely filled.

Hyper spectra show additional peaks in the region of >320 nm. These types of spectra are observed for main group elements with lower oxidation states such as Sn(II), and in transition metals with d^{1-6} (e_g levels only partially filled) and stable lower oxidation states like Mn(III). Here, the additional peaks are thought to arise from charge transfer effects.

5.2 Infrared Spectra

Historically, assignments of the vibrational bands in porphyrins have largely been made empirically, by comparing the IR spectra of different chemically well-defined structures with one another and finding correlations between them. Group vibrations were typically elucidated by comparison with smaller molecules for which group vibrations are commonly known. Deuteration methods have also been used, as these severely shift the absorption band of the respective bond[2]. With the rise of computational chemistry, IR spectra could also be calculated by means of normal coordinate analysis (carried out by solving the secular equations arising from the Schrödinger equation) using various kinds of force fields.
Vibrations in the porphin skeleton include N–H, C_{meso}–H, C_β–H and various collective vibrations that lead to ring deformations. For metal porphins that exhibit D_{4h} symmetry [28], 26 vibrations are IR-active (18 in-plane and 8 out-of-plane), whereas 39 are Raman-active (27 in-plane, 12 out-of-plane).

5.3 Mass Spectra

Mass spectra of porphyrins are fairly straightforward in that electron ionization typically leads to changes in the substituents and not at the porphyrin core. Even for metalloporphyrins, loss of the metal atom is rarely observed but rather, additional ligands are lost (if there are any). Hence, the most prominent observed peak is usually M^+, with M^{2+} occasionally being observed as well. In the case of OEP for example, ionization under EI-MS conditions leads to the consecutive fragmentation of ethyl groups (CH_3 loss, C_2H_5 loss etc.). The same behavior is observed for the Magnesium(II) complex and the Cobalt(II) complex.

[2]Deuteration can be achieved by refluxing the compound in deuterated protic solvents such as D_2O and/or TFA-*d*. For an example, see [27].

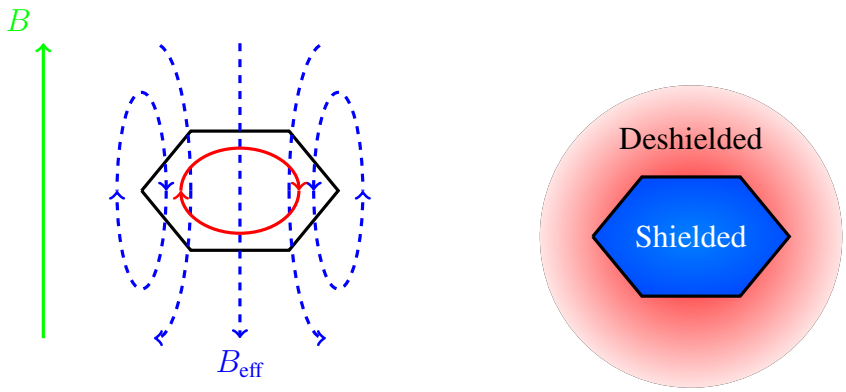

Figure 13: *Left:* Benzene (a six-membered cyclic polyene) subjected to a magnetic field (green) under NMR conditions. The induced ring current is shown in red, the effective secondary magnetic field is shown in blue. *Right:* The corresonding areas of the ring that experience shielding and an NMR upfield shift, or deshielding and a downfield shift. In the case of free-base porphyrins, the pyrrolic N–H protons are inside the macrocycle, thus being shielded and experiencing a upfield shift.

5.4 ^{1}H-NMR Spectra

Here, the spectra of porphyrins are similarly straightforward, owing to the aromatic nature of the porphyrin structure.

In all porphyrins, the pyrrolic N–H protons in the free-base porphyrins are substantially shifted towards the upfield, while the *meso*-protons are shifted towards the downfield. This phenomenon is explained schematically in Figure 13: A cyclic polyene subjected to a magnetic field under NMR conditions will induce a ring current in accordance with Lorentz' law. This current then gives rise to a secondary magnetic field that can point along the primary field (outside of the ring) or opposite to it (inside the ring). If nuclei are located on the inside of the ring, they experience an effective shielding from the external field and thus are shifted upfield relative to TMS. If they are located outside the ring structure, the effective field points parallel to the external one and deshields the nuclei, thus causing a downfield shift.

In the case of free-base porphyrins, the pyrrolic N–H protons are inside the macrocycle, so they are shielded and experience a upfield shift. In all porphyrins, they are found in the region between –3 ppm and –4 ppm. Note the significant shift,

for example in the case of porphin with –3.16 ppm [29], compared to the typical chemical shift of N–H in pyrrole in the positive double-digits.
In substituted porphyrins, this ring current similarly leads to deshielding of substituent-bonded protons, with the ring current effect decreasing as the nuclei located further away from the ring (see also the below figure). One prominent example is OEP, where the methylene resonances can be found at 4.14 ppm (quartet) and the methyl resonances – experiencing a weaker ring current effect – can be found at 1.95 ppm (triplet) [30].
This effect can be modulated by introducing different electron-donating or electron withdrawing groups into the molecule, as these can either increase or decrease the ring current effect, respectively. In the case of electron withdrawing groups, the deshielding effect from the groups themselves is overcompensated by the decreased ring current, leading to a net shielding.
Moreover, introduction of bulky substituents like *tert*-butyl groups causes a deviation of the porphyrin structure from planarity. This nonplanarity leads to a decreased π-π overlap and thus significantly reduces the ring current and any associated shielding and deshielding effects. The most striking example it the *tert*-butylporphyrin itself: Here, the N–H protons are found at 1.52 ppm, the methyl groups at 2.01 ppm, and the methine groups at 9.08 ppm [31]. This concept is further supported by the case of the porphin dication [32], whose pyrrolic protons experience an upfield shift towards -4.40 ppm, as the higher resonance stabilization leads to an increase in ring currents.
Chelation of a metal ion – although representing a perturbation to the π electron system as mentioned earlier – does not change the NMR spectra significantly: As can bee seen from the results of Buchler *et al.* for the example of OEP in Table 2, the changes in chemical shifts are seemingly minor with <0.3 ppm [33]. Moreover, the choice of the ligand (for otherwise coordinatively unsaturated complexes) does not induce any meaningful changes. There are, of course, exceptions to this rule in the form of paramagnetic complexes with $S \geq 1/2$. Their treatment is beyond the scope of this manuscript. However, one might consult literature such as chapter two of "The Porphyrins. Physical Chemistry, Part B" by David Dolphin.

Table 2: ^{1}H NMR shifts of some metallated OEP complexes, in $CDCl_3$ and referenced to TMS as internal standard. After Buchler *et al.*, data for porphin (metal H_2) from Inhoffen *et al.*

Metal	***meso*-CH**	**CH_2**	**CH_3**	**Ligand**
H_2	10.18	4.14	1.95	—
Al(III)	10.31	4.14	1.86	$–OC_6H_5$
Al(III)	10.38	4.13	1.94	$–OCH_3$
Al(III)	10.20	4.09	1.91	–OH
Ga(III)	10.13	4.05	1.87	$–OC_6H_5$
In(III)	10.30	4.14	1.95	$–OC_6H_5$
Si(IV)	9.85	4.14	1.99	$(–OCH_3)_2$
Si(IV)	10.07	4.12	1.90,1.93	$(–OC_6H_5)_2$
Ge(IV)	10.36	4.17	1.98	$(–OCH_3)_2$
Ge(IV)	10.30	4.15	1.93	$(–OC_6H_5)_2$
Sn(IV)	10.40	4.20	2.01	$(–OCH_3)_2$
Sn(IV)	10.32	4.15	1.93	$(–OC_6H_5)_2$

6 Reactivity of the Porphyrin Ring

For the most part, reactions of porphyrins take place at the peripheral substituents and not at the ring. However, the reactions that take place at the ring itself are mostly governed by its aromaticity.

6.1 Electrophilic Aromatic Substitution (S_EAr)

One of these aromaticity-typical recations is the electrophilic aromatic substitution. Here, Samuels *et al.* investigated the reactivity towards halogenation with Cl, Br, I of porphin [34]. Direct chlorination gave very low yields, bromination with *N*-bromosuccinimide (NBS) gave both monobrominated products; one at *meso*-position and one at the β-position. Iodine in chloroform gave no reaction and a mixture of I_2/KI/H_2SO_4 destroyed the porphin. As is expected for aromatic compounds, halogenation deactivates the ring inductively and activates it by resonance. Similarly, nitration of porphin leads to only monosubstitution to give the green nitroporphin with substitution strictly at the *meso*-position [35]. This reaction can easily be tracked with the bare eye, as the color of the mixture over time changes from red (porphin) to blue (porphin dication) to green (mononitroporphin). NMR

and UV/vis analysis showed that the product of further nitration has its second nitro group at the neighboring *meso*-position.
As Fuhrop *et al.* argued in the case of OEP [36], electropositive porphyrin rings should easily undergo oxidation or electrophilic addition reactions. This electropositivity can be imposed by complexation with a very electropositive metal. And indeed, their work found that copper and nickel complexes are especially sensitive towards Vilsmeyer-Haack formylation [30], leading only to the mono-*meso*-substituted product.

6.2 Nucleophilic Aromatic Substitution (S_NAr)

The toolbox of S_NAr reactions is limited to organometallic reagents, such as *n*-butyllithium, *n*-hexyllithium or phenyllithium. Apparently, sterically unhindered organometallics have an easier time reacting, with higher yields and less equivalents being needed [17]. In all cases, the reaction proceeds via nucleophilic attack at the *meso*-position, with the anionic intermediate carrying the negative charge at the opposite *meso*-position. Quenching with water and oxidation with DDQ then leads to the monoalkylated product. 5,10-disubstitution is accessible by using higher equivalents of the organometallic reagent.

6.3 Ring Cleavage

Going back to the work of Fuhrop *et al.*, the same argument about electropositivity was made with regards to photooxidation. Here, especially electropositive metals would be needed, such as magnesium, calcium or zinc. While there are no records about the reactivity of any calcium complexes (likely due to its the previously mentioned stability class), magnesium and zinc complexes of OEP have been found to be reactive. As a means towards a biomimetic analog of heme catabolism, oxidation of iron complexes of OEP has been tried in the past as well.
Both of these reactions led to bilindiones and biliverdins, respectively. They are treated in detail in the next chapter.

7 Bilindiones and Biliverdins

These classes of molecules differ from the porphyrins in that their π electron system is discontinuous and as established earlier, they are typically a product of heme catabolism, with verdoheme (a 5-oxaporphyrin) and *meso*-hydroxyporphyrin as intermediates. In experiments with Fe^{II} octaethylporphyrin, molecular oxygen and ascorbic acid as a model system for heme, it was observed that this oxidation process affects both the ligand and the iron atom (by oxidation to Fe^{III}). This lead to the name of *coupled oxidation* for the process of bilindione formation.
In the case of plants with their magnesium-coordinating chlorophyll structure, the porphyrin macrocycle is cleaved by ambient air to give a formylbiliverdin. In contrast to the previously mentioned reaction devised by Fuhrop *et al.*, the chlorophyll loses its magnesium atom prior to ring cleavage. This reaction, catalyzed by the enzyme *Mg dechelatase* and leading to pheophorbide a, is then followed by the actual oxidation by *pheophorbide a oxidase*.
Despite their different origin in humans and plants, both the biliverdins and the bilindiones share the commonality of being inherently helical molecules. This is caused both by the preference for an *all-Z* conformation (even in the absence of a coordinating metal atom) and a steric repulsion of the end groups in the tetrapyrrole structure [37][38].
As both a blessing and a curse, the literature situation for both bilindiones and biliverdins (involving man-made molecules and reactions) is more "manageable": On the one hand, this means that it is easier to keep up with new developments. On the other hand, it also means that there is less development in the first place if one is mostly concerned with their chemical and physical rather than their biological and physiological properties.

7.1 Bilindiones

While both bilindiones and biliverdins are theoretically accessible via subsequent MacDonald condensations, the most practical approach to obtain bilindiones to date seems to be a biomimetic reaction to the coupled oxidation that is found in nature. In the case of iron porphyrins as a starting material, the complex is typically

dissolved in CH_2Cl_2, $CHCl_3$ or MeOH, along with an excess of ligand (cyanide or pyridine) and ascorbic acid as a reducing agent. At ambient temperature and with exposure to air, the mixture is then subjected to vigorous stirring and the resulting product is washed and characterized with relative ease. This procedure has been most thoroughly studied with octaethylporphyrin (OEP). As the resulting bilindionato ligand is four-coordinating and three-protonic, the most well-studied metal atoms for complexes are Co [39], Ni [40], Cu [41], Fe [42], Mn [39] and – to a lesser extent – Pd [43].

In 2016, Mizutani *et al.* elucidated the reaction mechanism for the coupled oxidation conducted on FeTPP, a porphyrinato complex bearing phenyl groups in all *meso*-positions [44]. In this particular case, two different products are formed simultaneously, namely a biladienone and a bilindione. Using $^{18}O_2$ as the source of oxygen, they found that in the further case, the oxygen atoms in the two carbonyl functions stem from *one* dioxygen molecule, whereas in the latter, they are the result of *two* dioxygen molecules. Consequently, the authors argue, the coupled oxidation process in this case must involve a first oxidation step to give the biladienone, followed by a second step that gives the bilindione. Moreover, the biladienone may be converted into a bilatrienone by acid-catalyzed dehydration. Lastly, studies on the reactivity for TPP derivates in the same paper revealed that electron-donating groups in *para*-position favor the formation of the biladienone, whereas electron-withdrawing groups in the same position favor the formation of the bilindione.

Metal-bilindiones may also show a rich coordination chemistry, depending on the metal ion that is incorporated. The complex of Mn(III) with octaethylbilindione for example, actually exists as a dimer $\{Mn^{III}(\mu\text{-OEB})\}_2$, the structure is shown in Figure 14: Here, the manganese atoms are five-coordinate with four coordination sites being occupied by the nitrogen atoms of their own bilindione ligand, and the last one is occupied by the oxygen atom of the second monomer.

The resulting dimer is has a 1:1 stochiometry between ligand and metal, and is chiral. However, the compound crystallizes as a racemate. Dissolving this compound in pyridine leads to dimer cleavage, and the vacant fifth coordination site of manganese is then occupied by a pyridine ligand. This way, the complex

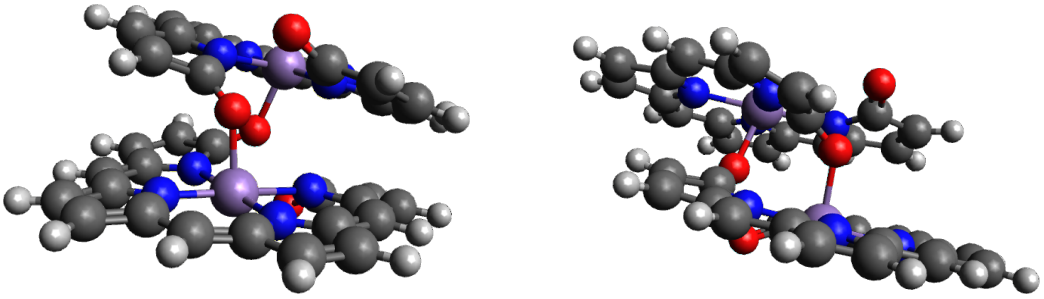

Figure 14: Structure of the complex $\{Mn^{III}(\mu\text{-OEB})\}_2$. Ethyl groups have been replaced by hydrogens for clarity.

Mn(OEP)(py) may be obtained. The same behavior [45] is found in the case of Fe^{III}, where the corresponding complex is $\{Fe^{III}(\mu\text{-OEB})\}_2$.
The case of palladium is even more interesting, as the tendency of this metal to coordinate π bonds comes into play. Treatment of OEB with palladium salts can lead to the tetranuclear complex $\{Pd_2(\mu\text{-OEB})\}_2$, whose structure is shown in Figure 15.

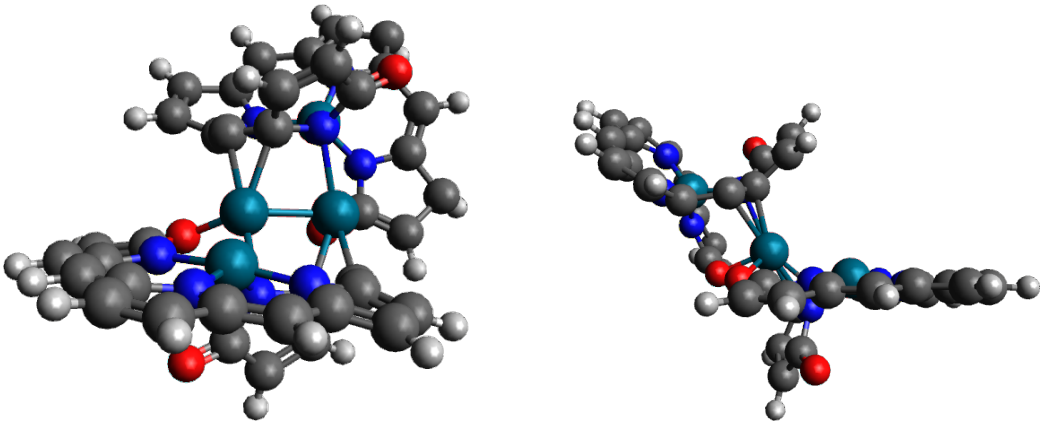

Figure 15: Structure of the complex $\{Pd_2(\mu\text{-OEB})\}_2$. Ethyl groups have been replaced by hydrogens for clarity.

This complex is again a dimer, but is bridged by a $(Pd^{I}_2)^{2+}$ unit, where each atom coordinates to a double bond of one OEB ligand. This coordination activates the double bonds, thus enabling a reaction with iodine in the presence of pyridine [46], as shown in Figure 16.

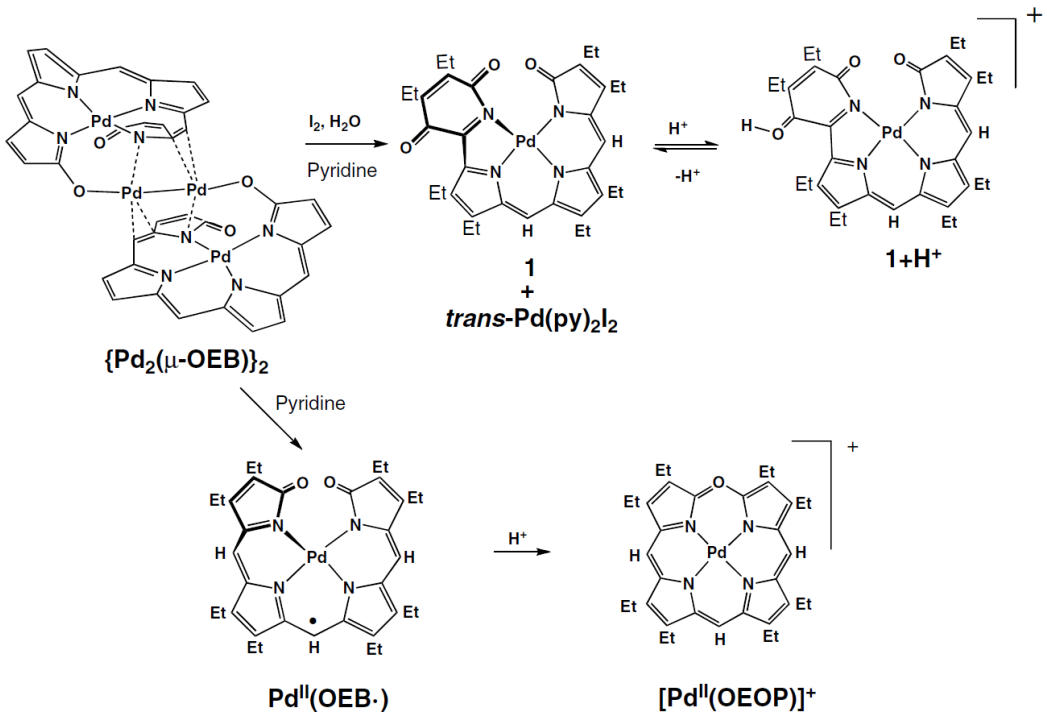

Figure 16: Reactions of $\{Pd_2(\mu\text{-OEB})\}_2$.

7.2 Biliverdins

As mentioned previously, this class of molecules might be most easily prepared by the photooxidation of magnesium porphyrins under ambient conditions. Using, OEP as a ligand, it was found that the OEFB complex is the sole reaction product. In their publications, Fuhrop *et al.* attribute this to the higher oxidization potential of the products. At the same time, the authors found, this complex is immensely labile towards any acids so that any eventual separation, even on desactivated Al_2O_3, is unsuccessful. One decomposition product that can be observed is especially striking, as its green color might indicate loss of Mg to give the green H_2OEFB free base. This however, has to date only been hypothesized and not investigated. The Mg(OEFB) complex can be transmetalated [47], such as with Co, Ni and Cu. These complexes seemingly have a lower oxidization potential when compared to Mg, as Balch *et al.* reported a differing stability when stored over long periods of time.

7.3 Properties

Using $ZnCl_2$, biliverdins may be converted into the corresponding Zn(Cl) 5-oxaporphyrins where the Zn^{II} atom is five-coordinate [48]. The resulting closed ring structure can then be opened up again by the use of different nucleophiles (such as amines, thiols or alcohols) to extend one end of the tetrapyrrole structure by a variety of functional groups [49].

Co [39], Ni [40], Cu [41] and Pd [50] complexes of octaethylbilindione are isostructural and – evidenced by infrared spectroscopy – involve an oxidized ligand, leading to the formulation of $M^{II}(OEB^{\cdot})$ rather than $M^{III}(OEB)$. In the case of Ni and Pd as central atoms, the complexes show the presence of free radical ligands, as evidenced by electron spin resonance experiments (with the gyromagnetic factor $g = 2.03$ for the Ni and $g = 2.08$ for the Pd complex [50][3]). In the light of these findings, the OEB ligand can be classified as *non-innocent*, meaning that upon coordination of a metal atom, (a) precise determination of its (physical, not formal!) oxidation state becomes impossible and (b) charge-transfer behavior is observed. The same appears to be true for the biliverdins, as indicated by a DFT survey by Wasbotten *et al*[51]. Here, the complex of iron(III) with unsubstituted formylbiliverdin and an additional chloridoligand – $[Fe^{III}(Blv)Cl]$ – is predicted to be a high-spin complex in its ground state with $S = 5/2$. The complexes of OEB with Co, Ni, Cu and Pd undergo redox reactions with the determined potentials given in Figure 17 below.

Solutions of Co(OEB) and Cu(OEB) are sensitive to air in that they undergo further oxidation with a second cleavage of the OEB ligand. In this case, two monoanionic ligands of *tetraethyl-propentdyopent* (TEPD) are formed – in the case of Co in 40 % yield. The structure of these complexes vaguely resembles a propeller shape, thus retaining the motif of helicity. Whether this oxidation proceeds towards complexes with four individual ligands is currently unknown.

Looking at both empirical and *ab initio* findings – empirical for OEB and *ab initio* for the biliverdins –, it seems that the non-innocence of both ligands arises from the steric repulsion of the oxygen atoms at each end group. Wasbotten *et al.* argue

[3] compared to, for example, $g \approx 2$ for the electron, ≈ 5.6 for the proton and ≈ -3.8 for the neutron.

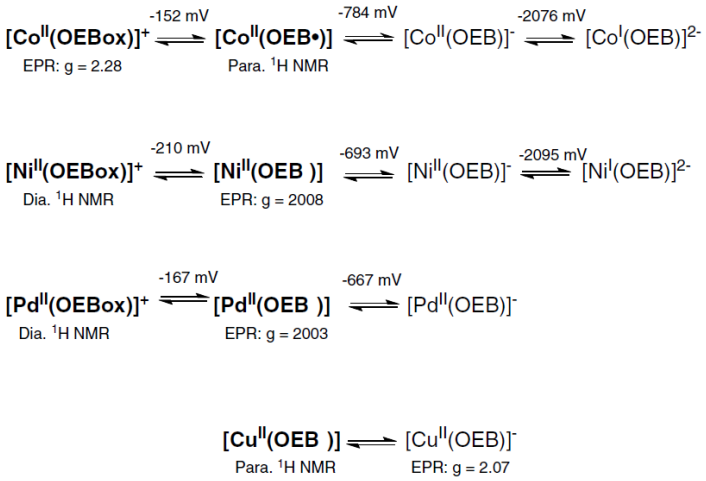

Figure 17: Redox potentials of M^{II}(OEB) with M = Co, Ni, Cu, Pd. Complexes that were isolated and characterized by x-ray diffraction are given in bold. "Para." and "Dia." denote a paramagnetic or diamagnetic ^{1}H NMR spectrum, respectively. Potentials are given in CH_2Cl_2 solution, with reference to ferrocene/ferrocinium.

that the deviation from planarity would lead to longer N–M bond distances that would stabilize the oxidation states of high-valent metals [51].

Just as the OEP complex of magnesium, the respective TPP complex may also undergo photooxidation. However, the reaction product here is not a formylbiliverdin: As the corresponding methine C–H bonds are instead C–Ph bonds, the resulting product is a bilindione with one benzaldehyde group. The resulting complex, a tetraphenylketobiliverdin (TPKB), can again be transmetalated with a metal acetate such as $Cu(OAc)_2$, as shown below.

8 Current Trends in Porphyrin Science

8.1 Molecular Electronics

8.1.1 Biladienones as Molecular Switches

The previously mentioned, bilindiones and biliverdins can be considered as molecular switches due to their ability to isomerize under irradiation with light. In 2006 [52], the Mizutani group in Kyoto used a zinc biladienone (a structure closely re-

lated to bilindiones where one methylene group is sp^3-hybridized instead) bearing an 4-(*n*-dodecyl)phenyl groups at all *meso*-positions to fabricate a molecular field-effect switch (FES). Upon adsorption on a gold layer (with SiO_2 as the underlying substrate), IR reflection absorption spectroscopy revealed that this molecule is lying flat on the surface so that the helical structure is retained and the molecular helix is sitting perpendicular to the surface plane. The biladienone was then sandwiched between two gold electrodes (source and drain) in a typical source-drain-gate setup, and the distance between source and drain was varied while measuring the conductance between them – both with and without applied gate voltage. In the absence of gate voltage, the measured conductance was steady and did not depend on the distance between both electrodes. Moreover, when a gate voltage was applied, the conductance sank as the distance between source and drain decreased. The same FES based on the biladienone without the alkyl chains did not show this behavior and instead, the conductance in the presence of gate voltage was steady. Consequently, the authors argue that the alkyl chains must play a vital role in this switching mechanism. This switching is supposedly caused by the molecules reversibly separating from the electrode via a conformational change that in turn leads to a change in the molecule's permanent dipole direction and density of states. However, it is worth pointing out that this zinc biladienone was incorporated into the FES *as a racemate*: any effects arising from a previous enantioseparation, such as a spin-polarized current, were not explored.

The orientation of this molecule together with its helical shape and conformational flexibility might make biladienones (and by extension, bilindiones and biliverdins) a promising candidate for exploration of the CISS effect. Moreover, as both the metal atom and the substituents can be varied with ease, helical tetrapyrroles like these may become a good "benchmark" platform, as one may vary the electronic and geometric structure without changing the underlying structural motif. This benchmark approach may then one day be helpful in constructing a quantitative and concise model of the CISS effect which does not exist to date. Laying the groundwork for this benchmark approach is the goal of this manuscript's author.

8.1.2 Vanadyl Porphyrins as Qubits

Quantum bits (often called *qubits*) are systems that can be described by quantum mechanics and that exist in only two easily distinguishable quantum states. As such, they provide the basis for enabling quantum computing and pushing the well-known Moore's Law. An essential parameter for what constitutes a "good" qubit candidate then has to be *spin coherence time* T_2 for which a system stays in a given quantum state – before succumbing to the process of *decoherence*.
The vanadyl ion VO^{2+} is one of these candidates for a versatile qubit. However, building an actual quantum chip requires the incorporation of this molecule in a very precise manner, and in the direct orientation. Otherwise, selectively manipulating quantum states becomes impossible. Moreover, these qubits would then need to be "wired up" to an electronic device, which might have implications for the spin coherence time. Hence arises the need for a carrier molecule, perhaps in the form a metal-organic framework (MOF).
In their 2020 publication, Urtizberea *et al.*[53] used 5,10,15,20-tetrakis(4-carboxyphenyl)-porphyrin as a carrier molecule. Using Zn(II) from $ZnCl_2$ as a linker for the carboxy groups, these individual qubits could then be ordered into a MOF under aqueous conditions. By grafting this framework onto a superconducting resonator (Nb on a sapphire wafer), microwave transmission, EPR and ac susceptibility measurements showed a spin coherence time of $T_2 > 10\,\mathrm{ns}$ and a spin-lattice relaxation time of $T_1 > 10\,\mathrm{ms}$ at $6\,\mathrm{K}$.

8.2 Structural Chemistry: Nonplanar Porphyrins

As briefly mentioned previously, the assumption was that cyclic tetrapyrroles (here, the porphyrins) are planar does not always hold true. In fact, in naturally occuring porphyrins as well as man-made porphyrins, it was found that certain substitution patterns can lead to considerable nonplanarity.
The most prominent researcher in this field of nonplanar porphyrins might be M. O. Senge, who is now teaching in Dublin. One of the molecules he investigated, namely octaethyl-tetraphenylporphyrin (H_2OETTP), showed considerable deviations from planarity in a complex with Cu(II) by assuming a saddle-conformation. Similarly, the tetra-*tert*-butyl-porphyrin mentioned previously showed the most

considerable distortion to date, as determined by theoretical calculations (the mo-lecule itself still has to be crystallized).
As this nonplanarity means a deviation of the sp^2-hybridized carbon's geometry from the "ideal", the π-aromatic system is destabilized due to a smaller p_π-p_π overlap of the participating carbon atoms. This *exercise in molecular gymnastics*, as Senge calls it in his 2006 review [54], leads to a plethora of interesting effects: bathochromic shifts of the absorption bands, easier oxidation, lower fluorescence yields, larger Stokes shifts, shorter lifetimes of the lowest excited states, faster intersystem crossing and internal conversion [55] are just some. Earlier in 2021, a computational tool [56] for nonplanarity prediction was published, which will hopefully help the field gain even more traction.

8.3 Catalysis: Carbene Transfer Reactions

As porphyrins are found in nature as part of the active sites of many enzymes (i.e., nature's own catalysts), it comes as no surprise that catalytic chemists are seeking to employ the underlying porphyrin heterocyclic structure to their own means. As one example, iron(III) tetraphenylporphyrin chloride (FeTPPCl) can be used in the C-H functionalization of various $C(sp^3)$-H bonds by using diazoalkanes with an electron withdrawing group such as -CN or $-CF_3$. This diazoalkane reacts with the porphyrin catalyst where it is then bonded in the form of a carbene and transferred to the target molecule. Stereoselective versions of this general reaction mechanism have been reported. An exemplary paper serving as a brief summary of available reactions can be found in [57].

8.4 Nonlinear Optics of Tetraphenylporphyrin

As seen previously, one of the intriguing features about porphyrins is that their macrocycle is quite readily accessible to electronic and topological modifications, and that these modifications can have enormous impact on their optical spectra. In combination with their thermal stability, it should come as no surprise that physicists are investigating this class of compounds as candidates for nonlinear optical applications. Moreover, the nonlinear optical effects (such as high harmonic or sum frequency generation) in organic molecules like porphyrins arise from

electronic polarization – a very fast effect, compared to the lattice distortions that inorganic materials rely on. Hence, they exhibit a shorter *nonlinear response time*.

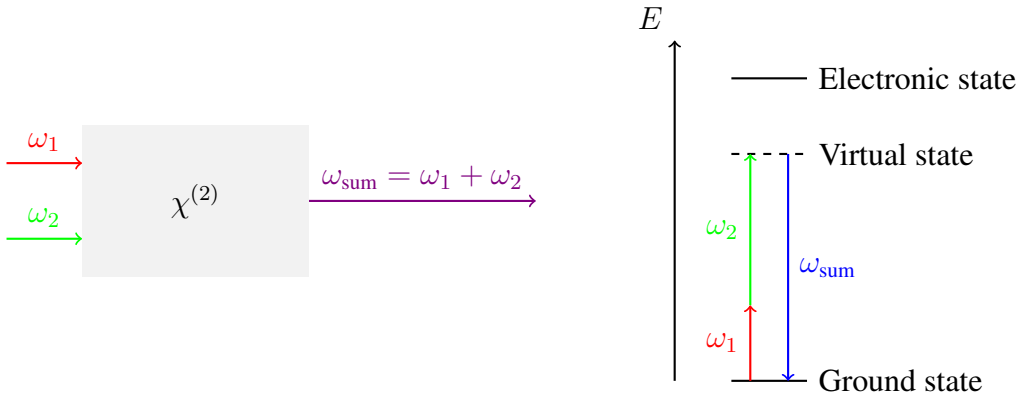

Figure 18: *Left*: Schematic representation of sum frequency generation (SFG), a second-order nonlinear phenomenon. Light of two frequencies ω_1 and ω_2 is irradiated onto a material with a nonzero second-order susceptibility to give reflected light $\omega_{\text{sum}} = \omega_1 + \omega_2$. *Right*: Energy diagram of the states involved in SFG.

The structurally very simple and thus easy to synthesize TPP was the first porphyrin to ever be investigated in terms of nonlinear parameters. Since that study in 1985 [58], a plethora of similar research followed, employing the use of different substituents at the phenyl groups, π-conjugating linker molecules, push-pull-systems, porphyrin arrays and the like.

In the case of TPP complexes with tetravalent metals, for example, it was found that the third-order nonlinear susceptibility $\chi^{(3)}$ (leading to stronger third order effects) is increased by as high as one order of magnitude when said metal carries a strongly electronegative axial ligand [59]. Another study later surveyed the nonlinear response times of TPP complexes with 16 different metals and found values in the realm of ps and ns [60]. Looking at the porphyrin itself rather than the role of the metals, Kandasamy *et al.* found that second order nonlinear effects (second harmonic generation, sum frequency generation etc.) are amplified if the phenyl groups carry strongly electron-donating groups in the *ortho*-position.

For an introduction into the field of nonlinear optics, see for example Boyd's *Nonlinear Optics* or Teich's and Saleh's *Fundamentals of Photonics* (herein especially

chapter 19). For a review article of porphyrins in nonlinear optics, see for example reference [61].

References

[1] Fischer, H., Orth, H. Die Chemie des Pyrrols, volume 1. Akademische Verlagsgesellschaft Leipzig, 1934

[2] Fischer, H., Orth, H. Die Chemie des Pyrrols, volume 2. Akademische Verlagsgesellschaft Leipzig, 1937

[3] Fischer, H., Orth, H. Die Chemie des Pyrrols, volume 2. Akademische Verlagsgesellschaft Leipzig, 1940

[4] American Chemical Society. Definitive Rules for the Nomenclature of Amino Acids, Steroids, Vitamins, and Carotenoids **82**, 21, 5575, 1960

[5] Shemin, D. From Cyclotrons to Cytochromes, chapter From Glycine to Heme, 117–129. Academic Press London/New York, 1982

[6] Stryer, Lubert. Biochemistry. W. H. Freeman, New York, 1988

[7] Senge, Mathias O., Sergeeva, Natalia N., Hale, Karl J. Classic highlights in porphyrin and porphyrinoid total synthesis and biosynthesis **50**, 7, 4730, 2021

[8] Eschenmoser, Albert. Corrin Syntheses. Part I **98**, 11-12, 1483, 2015

[9] Nicolaou, K. C., Vourloumis, Dionisios, Winssinger, Nicolas, Baran, Phil S. The Art and Science of Total Synthesis at the Dawn of the Twenty-First Century. Angewandte Chemie International Edition **39**, 1, 44, 2000

[10] Thudichum, JLW. Report on researches intended to promote an improved chemical identification of disease. 10th Report of The Medical Officer 152–233, 1867

[11] Fischer, Hans, Gleim, Wilhelm. Synthese des Porphins **521**, 1, 157, 1936

[12] Krol, Stefan. Notes- A New Synthesis of Porphin **24**, 12, 2065, 1959

[13] Ellis, Paul E., Langdale, Wayne A. Novel Biphasic Synthesis of Porphyrin. Journal of Porphyrins and Phthalocyanines **01**, 03, 305, 1997

[14] Taniguchi, Shozo. A Facile Route to Tripyrrane from 2,5-Bis(hydroxymethyl)pyrrole and the Improved Synthesis of Porphine by the "3 + 1" Approach **1999**, 1, 73, 1999

[15] Neya, Saburo, Funasaki, Noriaki. meso-Tetra(tert-butyl)porphyrin as a precursor of porphine **43**, 6, 1057, 2002

[16] Lindsey, Jonathan S., Schreiman, Irwin C., Hsu, Henry C., Kearney, Patrick C., Marguerettaz, Anne M. Rothemund and Adler-Longo reactions revisited: synthesis of tetraphenylporphyrins under equilibrium conditions **52**, 5, 827, 1987

[17] Senge, Mathias O., Davis, Mia. Porphyrin (porphine) — A neglected parent compound with potential **14**, 07, 557, 2010

[18] Sessler, Jonathan L., Mozaffari, Azadeh, Johnson, Martin R. 3,4-Diethylpyrrole and 2,3,7,8,12,13,17,18-Octaethylporphyrin **70**, 68, 1992

[19] Nguyen, Liem T., Senge, Mathias O., Smith, Kevin M. Simple Methodology for Syntheses of Porphyrins Possessing Multiple Peripheral Substituents with an Element of Symmetry **61**, 3, 998, 1996

[20] Arsenault, G. P., Bullock, E., MacDonald, S. F. Pyrromethanes and Porphyrins Therefrom1 **82**, 16, 4384, 1960

[21] Chantrell, S.J., McAuliffe, C.A., Munn, R.W., Pratt, A.C. The status of molecular orbital calculations on porphyrins and their complexes **16**, 4, 259, 1975

[22] Platt, John R. Classification of Spectra of Cata-Condensed Hydrocarbons **17**, 5, 484, 1949

[23] Barone, Vincenzo, Cossi, Maurizio. Quantum Calculation of Molecular Energies and Energy Gradients in Solution by a Conductor Solvent Model **102**, 11, 1995, 1998

[24] Gouterman, Martin. Spectra of porphyrins **6**, 138, 1961

[25] Gouterman, Martin, Wagnière, Georges H., Snyder, Lawrence C. Spectra of porphyrins **11**, 1-6, 108, 1963

[26] Edwards, Lawrence, Dolphin, David H., Gouterman, Martin. Porphyrins **35**, 1, 90, 1970

[27] Frampton, Michael J., Accorsi, Gianluca, Armaroli, Nicola, Rogers, Joy E., Fleitz, Paul A., McEwan, Kenneth J., Anderson, Harry L. Synthesis and near-infrared luminescence of a deuterated conjugated porphyrin dimer for probing the mechanism of non-radiative deactivation **5**, 7, 1056, 2007

[28] Ogoshi, Hisanobu, Saito, Yutaka, Nakamoto, Kazuo. Infrared Spectra and Normal Coordinate Analysis of Metalloporphins **57**, 10, 4194, 1972

[29] Solov'ev, K. N., Mashenkov, V. A., Gradyushko, A. T., Turkova, A. E., Lezina, V. P. High resolution nmr spectra of porphin and of porphin derivatives **13**, 2, 1106, 1970

[30] Inhoffen, Hans Herloff, Fuhrhop, Jürgen-Hinrich, Voigt, Hartmut, Brockmann, Hans. Zur weiteren Kenntnis des Chlorophylls und des Hämins, VI. Formylierung dermeso-Kohlenstoffatome von Alkyl-substituierten Porphyrinen **695**, 1, 133, 1966

[31] Senge, Mathias O., Bischoff, Ines, Nelson, Nora Y., Smith, Kevin M. Synthesis, Reactivity and Structural Chemistry of 5,10,15,20-Tetraalkylporphyrins. Journal of Porphyrins and Phthalocyanines **03**, 02, 99, 1999

[32] Abraham, R. J., Jackson, A. H., Kenner, G. W. 673. The proton magnetic resonance spectra of porphyrins. Part I. The effect of β-substitution on the proton chemical shifts of porphyrins **0**, 0, 3468, 1961

[33] Buchler, Johann Walter, Puppe, Lothar, Rohbock, Klaus, Schneehage, Hans Henning. Metall-Komplexe mit Tetrapyrrol-Liganden, VIII. Methoxo- und Phenoxo-metallkomplexe des Octaäthylporphins mit Zentralionen des Typs M^{3+}, M^{4-} und MO^{3-}; neue Wolfram- und Rheniumporphine **106**, 8, 2710, 1973

[34] Samuels, E., Shuttleworth, R., Stevens, T. S. Halogenation of porphin and octaethylporphin 145, 1968

[35] Drach, John E., Longo, Frederick R. Electrophilic substitution on porphin. I. Nitration **39**, 22, 3282, 1974

[36] Furhop, Jurgen H., Kadish, Karl M., Davis, Donald G. Redox behavior of metallo oxtaethylporhyrins **95**, 16, 5140, 1973

[37] Terry, Matthew J., McDowell, Michael T., Lagarias, J. Clark. (3Z)- and (3E)-Phytochromobilin Are Intermediates in the Biosynthesis of the Phytochrome Chromophore **270**, 19, 11111, 1995

[38] Sheldrick, William S. Crystal and molecular structure of biliverdin dimethyl ester , 13, 1457, 1976

[39] Balch, Alan L., Mazzanti, Marinella, Noll, Bruce C., Olmstead, Marilyn M. Coordination Patterns for Biliverdin-Type Ligands. Helical and Linked Helical Units in Four-Coordinate Cobalt and Five-Coordinate Manganese(III) Complexes of Octaethylbilindione **116**, 20, 9114, 1994

[40] Bonfiglio, Joseph V., Bonnett, Raymond, Buckley, Dennis G., Hamzetash, Dariush, Hursthouse, Michael B., Malik, K.M.Abdul, McDonagh, Antony F., Trotter, Jill. Linear tetrapyrroles as ligands **39**, 11, 1865, 1983

[41] Balch, Alan L., Mazzanti, Marinella, Noll, Bruce C., Olmstead, Marilyn M. Geometric and electronic structure and dioxygen sensitivity of the copper complex of octaethylbilindione, a biliverdin analog **115**, 25, 12206, 1993

[42] Rath, Sankar Prasad, Olmstead, Marilyn M., Latos-Grażyński, Lechoslaw, Balch, Alan L. Formation and Isolation of an Iron-Tripyrrole Complex from Heme Degradation **125**, 42, 12678, 2003

[43] Lord, Pamela, Olmstead, Marilyn M., Balch, Alan L. Tetrapyrroles as π Donors: A Pd_2^{2+} Unit Sandwiched between Two Helical Bilindione–Palladium Moieties. Angewandte Chemie International Edition **38**, 18, 2761, 1999

[44] Mizutani, Tadashi. Coupled oxidation of iron tetraarylporphyrins as a synthetic tool for linear tetrapyrroles **20**, 01n04, 108, 2016

[45] Balch, Alan L., Latos-Grazynski, Lechoslaw, Noll, Bruce C., Olmstead, Marilyn M., Safari, Nasser. Isolation and characterization of an iron biliverdin-type complex that is formed along with verdohemochrome during the coupled oxidation of iron(II) octaethylporphyrin **115**, 20, 9056, 1993

[46] Lord, Pamela A., Noll, Bruce C., Olmstead, Marilyn M., Balch, Alan L. A Remarkable Skeletal Rearrangement of a Coordinated Tetrapyrrole: Chemical Consequences of Palladium π-Coordination to a Bilindione **123**, 43, 10554, 2001

[47] Koerner, Richard, Olmstead, Marilyn M., Ozarowski, Andrzej, Phillips, Shane L., Calcar, Pamela M. Van, Winkler, Krzysztof, Balch, Alan L. Possible Intermediates in Biological Metalloporphyrin Oxidative Degradation. Nickel, Copper, and Cobalt Complexes of Octaethylformybiliverdin and Their Conversion to a Verdoheme **120**, 6, 1274, 1998

[48] Fuhrhop, Jürgen-Hinrich, Krüger, Peter, Sheldrick, William S. Darstellung, Struktur und Eigenschaften der 5-Aza-, 5-Oxonia-und 5-Thioniamesoporphin-dimethylester und -protoporphin-dimethylester **1977**, 3, 339, 1977

[49] Kakeya, Kazuhisa, Aozasa, Masakatsu, Mizutani, Tadashi, Hitomi, Yutaka, Kodera, Masahito. Nucleophilic Ring Opening of meso-Substituted 5-Oxaporphyrin by Oxygen, Nitrogen, Sulfur, and Carbon Nucleophiles **79**, 6, 2591, 2014

[50] Lord, Pamela A., Olmstead, Marilyn M., Balch, Alan L. Redox Characteristics of Nickel and Palladium Complexes of the Open-Chain Tetrapyrrole Octaethylbilindione: A Biliverdin Model **39**, 6, 1128, 2000

[51] Wasbotten, Ingar, Ghosh, Abhik. Biliverdine-Based Metalloradicals: Sterically Enhanced Noninnocence **45**, 13, 4914, 2006

[52] Matsui, E., Matsuzawa, N. N., Harnack, O., Yamauchi, T., Hatazawa, T., Yasuda, A., Mizutani, T. A New Molecular Switch Based on Helical Biladienone **18**, 19, 2523, 2006

[53] Urtizberea, Ainhoa, Natividad, Eva, Alonso, Pablo J., Pérez-Martínez, Laura, Andrés, Miguel A., Gascón, Ignacio, Gimeno, Ignacio, Luis, Fernando, Roubeau, Olivier. Vanadyl spin qubit 2D arrays and their integration on superconducting resonators **7**, 3, 885, 2020

[54] Senge, Mathias O. Exercises in molecular gymnastics—bending, stretching and twisting porphyrins , 3, 243, 2006

[55] Senge, Mathias, Ryan, Aoife, Letchford, Kristie, MacGowan, Stuart, Mielke, Tamara. Chlorophylls, Symmetry, Chirality, and Photosynthesis **6**, 3, 781, 2014

[56] Krumsieck, Jens, Bröring, Martin. PorphyStruct : A Digital Tool for the Quantitative Assignment of Non-Planar Distortion Modes in Four-Membered Porphyrinoids **27**, 45, 11580, 2021

[57] Weissenborn, Martin J., Koenigs, Rene M. Iron-porphyrin Catalyzed Carbene Transfer Reactions – an Evolution from Biomimetic Catalysis towards Chemistry-inspired Non-natural Reactivities of Enzymes **12**, 8, 2171, 2020

[58] Blau, W., Byrne, H., Dennis, W.M., Kelly, J.M. Reverse saturable absorption in tetraphenylporphyrins **56**, 1, 25, 1985

[59] Kandasamy, K., Shetty, Shankar J., Puntambekar, P. N., Srivastava, T. S., Kundu, T., Singh, Bhanu P. Non-resonant third-order optical non-linearity of porphyrin derivatives , 13, 1159, 1997

[60] Kandasamy, K., Shetty, Shankar J., Puntambekar, P. N., Srivastava, T. S., Kundu, T., Singh, Bhanu P. Effects of metal substitution on third-order optical non-linearity of porphyrin macrocycle. Journal of Porphyrins and Phthalocyanines **3**, 2, 81, 1999

[61] Senge, M. O., Fazekas, M., Notaras, E. G. A., Blau, W. J., Zawadzka, M., Locos, O. B., Ni Mhuircheartaigh, E. M. Nonlinear Optical Properties of Porphyrins **19**, 19, 2737, 2007

9 Supplementary Information

Periodic Table of Metalloporphyrins

Stability classes	
I	Not demetalated by conc. H_2SO_4
II	Demetalated by conc. H_2SO_4
III	Demetalated by conc. HCl
III	Demetalated by acetidc acid
V	Demetalated by water|
	See notes in caption.

H																	He
Li	Be											B	C	N	O	F	Ne
Na	Mg											Al	Si	P	S	Cl	Ar
K	Ca	Sc	Ti	V	Cr	Mn	Fe	Co	Ni	Cu	Zn	Ga	Ge	As	Se	Br	Kr
Rb	Sr	Y	Zr	Nb	Mo	Tc	Ru	Rh	Pd	Ag	Cd	In	Sn	Sb	Te	I	Xe
Cs	Ba	*	Hf	Ta	W	Re	Os	Ir	Pt	Au	Hg	Tl	Pb	Bi	Po	At	Rn
Fr	Ra	**	Rf	Db	Sg	Bh	Hs	Mt	Ds	Rg	Cn	Nh	Fl	Mc	Lv	Ts	Og

La	Ce	Pr	Nd	Pm	Sm	Eu	Gd	Tb	Dy	Ho	Er	Tm	Yb	Lu
Ac	Th	Pa	U	Np	Pu	Am	Cm	Bk	Cf	Es	Fm	Md	No	Lr

Table 3: Periodic table of metalloporphyrins, with colored entries for those elements whose stability classes were reported in porphyrin complexes. The here, the class is assigned based on overall tendencies for the different porphyrin ligands. *Note:* For the following elements, the stability class is dependent on oxidation state: Cr (Cr^{III} class I), Mn (Mn^{III} class II, Mn^{II} class IV), Fe (Fe^{II} class III, Fe^{III} class II).